

# Space-time least squares approximation for Schrödinger equation and efficient solver

Andrea Bressan<sup>b</sup>, Alen Kushova<sup>a,\*</sup>, Giancarlo Sangalli<sup>a,b</sup>, Mattia Tani<sup>a</sup>

<sup>a</sup>*Dipartimento di Matematica “F. Casorati”, Università di Pavia, Via A. Ferrata, 5, 27100 Pavia, Italy.*

<sup>b</sup>*Istituto di Matematica Applicata e Tecnologie Informatiche, “E. Magenes” del CNR, Via A. Ferrata, 1, 27100 Pavia, Italy.*

---

## Abstract

In this work we present a space-time least squares isogeometric discretization of the Schrödinger equation and propose a preconditioner for the arising linear system in the parametric domain. Exploiting the tensor product structure of the basis functions, the preconditioner is written as the sum of Kronecker products of matrices. Thanks to an extension to the classical Fast Diagonalization method, the application of the preconditioner is efficient and robust w.r.t. the polynomial degree of the spline space. The time required for the application is almost proportional to the number of degrees-of-freedom, for a serial execution.

*Keywords:* Isogeometric Analysis, splines, Schrödinger equation, space-time Least squares formulation, Fast Diagonalization.

---

## 1. Introduction

Space-time finite element methods originated in the papers [1, 2, 3, 4], where standard finite elements are ascribed an extra dimension for the time and, typically, adopt a discontinuous approximation in time, since this produces a time marching algorithm with a traditional step-by-step format (see e.g. [5]). Over the years, the theory of space-time methods has been developed mainly for evolutionary equations of the parabolic type and hyperbolic type, whereas, for quantum mechanics, and more precisely for Schrödinger’s equation, there are few contributions and the methods are still in development.

To our knowledge, one of the first works concerning space-time variational formulations for the (non-linear) Schrödinger equation, is [6], in which Karakashian and Makridakis proposed a space-time method combining a conforming Galerkin discretization in space and an upwind DG time-stepping. This method reduces to a Radau IIA Runge-Kutta time discretization in the case of constant potentials. In [7], for the linear Schrödinger equation the authors propose two variational formulations that are proved to be well posed: a strong formulation, with no relaxation of the original equation, and an ultraweak formulation, that transfers all derivatives onto test functions. The proposed discretization for the ultraweak form is based on a discontinuous Petrov-Galerkin (DPG) method, that addresses optimal stability, and quasi-optimal error rates in  $L^2$ -norm. In [8] a space-time ultraweak Trefftz discontinuous Galerkin (DG) method for the Schrödinger equation with piecewise-constant potential is proposed and analyzed, proving well-posedness and stability of the method, and optimal high-order  $h$ -convergence error estimates in a skeleton norm, for the one and two dimensional cases. Recently, in [9], Hain and Urban proposed a space-time ultraweak variational formulation with optimal inf-sup constant. The formulation in [9] is related to the ultraweak DPG method in [7], but differs in the choice of the test and trial spaces. Hain and Urban first fix a conforming test space, and then construct an optimal trial space, while Demkowicz et al. first constructs a trial space

---

\*Corresponding author

*Email addresses:* [andrea.bressan@imati.cnr.it](mailto:andrea.bressan@imati.cnr.it) (Andrea Bressan), [alen.kushova01@universitadipavia.it](mailto:alen.kushova01@universitadipavia.it) (Alen Kushova), [giancarlo.sangalli@unipv.it](mailto:giancarlo.sangalli@unipv.it) (Giancarlo Sangalli), [mattia.tani@unipv.it](mailto:mattia.tani@unipv.it) (Mattia Tani)

and then a suitable test space. The discretization proposed in [9] uses high order B-splines with maximum regularity and can be extended to the Isogeometric Analysis (IgA) framework.

Introduced in [10], see also the book [11], IgA, is an evolution of the classical finite element methods. In IgA, both the approximation of the solution of the partial differential equation that models the problem, and the representation of the computational domain, are accomplished using B-spline functions, or their generalizations (NURBS). This is meant to simplify the interoperability between computer aided design and numerical simulations. IgA also benefits from the approximation properties of splines, whose high-continuity yields higher accuracy when compared to  $C^0$  piecewise polynomials, see e.g., [12, 13, 14].

In this paper we focus on the linear time dependent Schrödinger equation without potential. Starting from the well posed space-time strong formulations in [7], we derive a well posed space-time isogeometric Petrov-Galerkin discretization, that is essentially a Galerkin approximation of the space-time least squares variational formulation of the model problem. The matrix associated to the discrete linear system can be written as sum of Kronecker products, and has the same structure of the one arising from [9]. The main contribution of this paper, is the development of a stable preconditioner that leads to a fast solver for the problem modeled in the parametric domain. As it was done in [15, 16] for parabolic problems, our preconditioner exploits the Kronecker structure of the linear system, and makes use of Fast Diagonalization method (FD) [17]. In this work, FD is applied among the space direction only. Although, the computational cost of the setup of the resulting preconditioner is  $O(N_{dof})$  Floating-Point operations (FLOPs), while its application is  $O(N_{dof}^{1+1/d})$  FLOPs, where  $d$  is the number of spatial dimensions and  $N_{dof}$  denotes the total number of degrees-of-freedom (assuming, for simplicity, to have the same number of degrees-of-freedom in time and in each spatial direction). We remark that global space-time methods, in principle, facilitate the full parallelization of the solver, see [18, 19, 20].

The outline of the paper is as follows. The model problem is introduced in Section 2. In Section 3 we present the basics of B-splines based IgA and the main properties of the Kronecker product operation. The isogeometric least squares discretization is introduced in Section 4, while in Section 5 we define the preconditioner for the parametric domain and we discuss its application. We present the numerical results assessing the performance of the proposed preconditioner in Section 6. Finally, in the last section we draw some conclusions and we highlight some future research directions.

## 2. Model problem

We consider a bounded domain  $\Omega \subset \mathbb{R}^d$ , usually  $d = 1, 2, 3$ , with Lipschitz boundary, and a time interval  $(0, T)$ , where  $T > 0$  is the final time. The space-time domain is denoted by  $\mathcal{Q} := (0, T) \times \Omega$ . Assuming Dirichlet boundary conditions, denote by  $\Gamma_D := (0, T) \times \partial\Omega$  the Dirichlet boundary of the space-time cylinder  $\mathcal{Q}$ , while  $\mathcal{Q}_0 = \{0\} \times \Omega$  is the initial side. Our model problem is the Schrödinger equation with homogeneous boundary and initial conditions: we look for a solution  $u$  such that

$$\begin{cases} i\partial_t u - \nu\Delta u = f & \text{in } \mathcal{Q}, \\ u = 0 & \text{on } \Gamma_D, \\ u = 0 & \text{in } \mathcal{Q}_0, \end{cases} \quad (2.1)$$

where  $i$  is the imaginary unit and  $\nu > 0$  is a constant coefficient usually depending on Planck's constant  $\hbar$  and the mass of the modeled physical particle. We assume that  $f \in L^2(\mathcal{Q})$  and denote by  $\mathbb{S} := i\partial_t - \nu\Delta$  the Schrödinger operator,  $\mathbb{S}^*$  its formal adjoint, and  $(\cdot, \cdot)$  the complex scalar product in  $L^2(\mathcal{Q})$ .

### 2.1. Space-time variational formulation

Let us introduce the Hilbert spaces

$$\begin{aligned} \mathcal{V} &:= \{v \in L^2(\mathcal{Q}) : \mathbb{S}v \in L^2(\mathcal{Q}) \text{ and } (\mathbb{S}^*w, v) - (w, \mathbb{S}v) = 0 \forall w \in C_0^\infty(\mathbb{R}^{d+1}) : w|_{\Gamma_D \cup (\{T\} \times \Omega)} = 0\}, \\ \mathcal{W} &:= L^2(\mathcal{Q}), \end{aligned}$$

endowed with the following norms

$$\|v\|_{\mathcal{V}}^2 := \|v\|_{L^2(\mathcal{Q})}^2 + \|\mathbb{S}v\|_{L^2(\mathcal{Q})}^2 \quad \text{and} \quad \|w\|_{\mathcal{W}} := \|w\|_{L^2(\mathcal{Q})},$$

respectively. Then, the space-time variational formulation of (2.1) reads:

$$\text{Find } u \in \mathcal{V} \text{ such that } \mathcal{A}(u, v) = \mathcal{F}(v) \quad \forall v \in \mathcal{W}, \quad (2.2)$$

where the sesquilinear form  $\mathcal{A}(\cdot, \cdot)$  and the linear form  $\mathcal{F}(\cdot)$  are defined  $\forall v \in \mathcal{V}$  and  $\forall w \in \mathcal{W}$  as

$$\mathcal{A}(v, w) := \int_{\Omega} \int_0^T (\mathbb{S}v) \bar{w} \, dt \, d\Omega \quad \text{and} \quad \mathcal{F}(w) := \int_{\Omega} \int_0^T f \bar{w} \, dt \, d\Omega.$$

The well-posedness of the variational formulation above, for  $d = 1$ , is in [7], but the generalization to  $d > 1$  is straightforward, see the Appendix of this paper.

## 2.2. Extensions

The previous setting can be generalized to non-homogeneous initial and boundary conditions. For example, suppose that in (2.1) we have the initial condition  $u = u_0$  in  $\mathcal{Q}_0$  with  $u_0 \in L^2(\Omega)$ . Then, we consider a lifting  $\underline{u}_0$  of  $u_0$  such that  $\underline{u}_0 \in L^2(\mathcal{Q})$ , see e.g. [21]. Finally, we split the solution  $u$  as  $u = \underline{u} + \underline{u}_0$ , where  $\underline{u} \in \mathcal{X}$  is the solution of the following Schrödinger equation with homogeneous initial and boundary conditions:

$$\begin{cases} i\partial_t \underline{u} - \nu \Delta \underline{u} = \underline{f} & \text{in } \mathcal{Q}, \\ \underline{u} = 0 & \text{on } \Gamma_D, \\ \underline{u} = 0 & \text{in } \mathcal{Q}_0, \end{cases}$$

where  $\underline{f} := f - \mathbb{S}\underline{u}_0$ .

## 3. Isogeometric framework and preliminaries

### 3.1. B-Splines

Given  $m$  and  $p$  two positive integers, a knot vector in  $[0, 1]$  is a sequence of non-decreasing points  $\Xi := \{0 = \xi_1 \leq \dots \leq \xi_{m+p+1} = 1\}$ . We consider open knot vectors, i.e. we set  $\xi_1 = \dots = \xi_{p+1} = 0$  and  $\xi_m = \dots = \xi_{m+p+1} = 1$ , and denote by  $Z = \{\zeta_1, \dots, \zeta_r\}$  the vector of breakpoints, that is the vector of knots without repetition.

Univariate B-splines  $\widehat{b}_{i,p} : (0, 1) \rightarrow \mathbb{R}$  are piecewise polynomials defined according to Cox-De Boor recursion formulas (see [22]). The univariate spline space is defined as

$$\widehat{\mathcal{S}}_h^p := \text{span}\{\widehat{b}_{i,p}\}_{i=1}^m,$$

where  $h$  denotes the mesh-size, i.e.  $h := \max\{|\xi_{i+1} - \xi_i| \mid i = 1, \dots, m+p\}$ . The interior knot multiplicity influences the smoothness of the B-splines at the knots (see [22]). For more details on B-splines properties and their use in IgA we refer to [11].

Multivariate B-splines are defined as tensor product of univariate B-splines. We consider functions that depend on  $d$  spatial variables and the time variable. Therefore, given positive integers  $m_l, p_l$  for  $l = 1, \dots, d$  and  $m_t, p_t$ , we introduce  $d+1$  univariate knot vectors  $\Xi_l := \{\xi_{l,1} \leq \dots \leq \xi_{l,m_l+p_l+1}\}$ , with associated breakpoints  $Z_l = \{\zeta_{l,1}, \dots, \zeta_{l,r_l}\}$ , for  $l = 1, \dots, d$  and  $\Xi_t := \{\xi_{t,1} \leq \dots \leq \xi_{t,m_t+p_t+1}\}$  with  $Z_t = \{\zeta_{t,1}, \dots, \zeta_{t,r_t}\}$ . Let  $h_l$  be the mesh-size associated to the knot vector  $\Xi_l$  for  $l = 1, \dots, d$ , let  $h_s := \max\{h_l \mid l = 1, \dots, d\}$  be the maximal mesh-size in all spatial knot vectors and let  $h_t$  be the mesh-size of the time knot vector. Let also  $\mathbf{p}$  be the vector that contains the degree indexes, i.e.  $\mathbf{p} := (p_t, \mathbf{p}_s)$ , where  $\mathbf{p}_s := (p_1, \dots, p_d)$ . For simplicity, we assume to have the same polynomial degree in all spatial directions, i.e., with abuse of notations, we set  $p_1 = \dots = p_d =: p_s$ , but the general case is similar.

We assume that the following local quasi-uniformity of the knot vectors holds.

**Assumption 1.** *There exists  $\theta \geq 1$ , independent of  $h_s$  and  $h_t$ , such that  $\theta^{-1} \leq \zeta_{l,i}/\zeta_{l,i+1} \leq \theta$  for  $i = 1, \dots, r_l$ ,  $l = 1, \dots, d$  and  $\theta^{-1} \leq \zeta_{t,i}/\zeta_{t,i+1} \leq \theta$  for  $i = 1, \dots, r_t$ .*

The multivariate B-splines are defined as

$$\widehat{B}_{\mathbf{i},\mathbf{p}}(\tau, \boldsymbol{\eta}) := \widehat{b}_{i_t, p_t}(\tau) \widehat{B}_{\mathbf{i}_s, \mathbf{p}_s}(\boldsymbol{\eta}),$$

where

$$\widehat{B}_{\mathbf{i}_s, \mathbf{p}_s}(\boldsymbol{\eta}) := \widehat{b}_{i_1, p_s}(\eta_1) \dots \widehat{b}_{i_d, p_s}(\eta_d), \quad (3.1)$$

$\mathbf{i}_s := (i_1, \dots, i_d)$ ,  $\mathbf{i} := (i_t, \mathbf{i}_s)$  and  $\boldsymbol{\eta} = (\eta_1, \dots, \eta_d)$ . The corresponding spline space is defined as

$$\widehat{\mathcal{S}}_h^{\mathbf{p}} := \text{span} \left\{ \widehat{B}_{\mathbf{i}, \mathbf{p}} \mid i_t = 1, \dots, m_t; i_l = 1, \dots, m_l \text{ for } l = 1, \dots, d \right\},$$

where  $h := \max\{h_t, h_s\}$ . We have that  $\widehat{\mathcal{S}}_h^{\mathbf{p}} = \widehat{\mathcal{S}}_{h_t}^{p_t} \otimes \widehat{\mathcal{S}}_{h_s}^{p_s}$ , where

$$\widehat{\mathcal{S}}_{h_s}^{p_s} := \text{span} \left\{ \widehat{B}_{\mathbf{i}_s, \mathbf{p}_s} \mid i_l = 1, \dots, m_l; l = 1, \dots, d \right\}$$

is the space of tensor-product splines on  $\widehat{\Omega} := (0, 1)^d$ . Finally, we make the following regularity assumption.

**Assumption 2.** *We assume that  $p_t \geq 1$ ,  $p_s \geq 2$  and that  $\widehat{\mathcal{S}}_{h_t}^{p_t} \subset C^0((0, 1))$  and  $\widehat{\mathcal{S}}_{h_s}^{p_s} \subset C^1(\widehat{\Omega})$ .*

### 3.2. Isogeometric spaces

The space-time computational domain that we consider is  $(0, T) \times \Omega$ , where  $T > 0$  is the final time and  $\Omega \subset \mathbb{R}^d$  is the space domain. The choice of considering the time as first variable will be clarified in Section 5.2. The following assumptions asserts the regularity of the parametrization.

**Assumption 3.** *We assume that  $\Omega$  is parametrized by  $\mathbf{F} : \widehat{\Omega} \rightarrow \Omega$ , with  $\mathbf{F} \in [\widehat{\mathcal{S}}_{h_s}^{p_s}]^d$  on the closure of  $\widehat{\Omega}$ . Moreover, we assume that  $\mathbf{F}^{-1}$  has piecewise bounded derivatives of any order.*

Denote by  $\mathbf{x} = (x_1, \dots, x_d) := \mathbf{F}(\boldsymbol{\eta})$  and  $t := T\tau$ . Then the space-time domain is given by the parametrization  $\mathbf{G} : (0, 1) \times \widehat{\Omega} \rightarrow (0, T) \times \Omega$ , such that  $\mathbf{G}(\tau, \boldsymbol{\eta}) := (T\tau, \mathbf{F}(\boldsymbol{\eta})) = (t, \mathbf{x})$ .

We introduce the spline space with initial and boundary conditions, in parametric coordinates, as

$$\widehat{\mathcal{X}}_{h,0} := \left\{ \widehat{v}_h \in \widehat{\mathcal{S}}_h^{\mathbf{p}} \mid \widehat{v}_h = 0 \text{ on } \{0\} \times \widehat{\Omega} \text{ and } \widehat{v}_h = 0 \text{ on } (0, 1) \times \partial\widehat{\Omega} \right\}.$$

Notice that  $\widehat{\mathcal{X}}_{h,0} = \widehat{\mathcal{X}}_{t, h_t, 0} \otimes \widehat{\mathcal{X}}_{s, h_s}$ , where

$$\begin{aligned} \widehat{\mathcal{X}}_{t, h_t, 0} &:= \left\{ \widehat{w}_h \in \widehat{\mathcal{S}}_{h_t}^{p_t} \mid \widehat{w}_h(0) = 0 \right\} = \text{span} \left\{ \widehat{b}_{i_t, p_t} \mid i_t = 2, \dots, m_t \right\}, \\ \widehat{\mathcal{X}}_{s, h_s} &:= \left\{ \widehat{w}_h \in \widehat{\mathcal{S}}_{h_s}^{p_s} \mid \widehat{w}_h = 0 \text{ on } \partial\widehat{\Omega} \right\} \\ &= \text{span} \left\{ \widehat{b}_{i_1, p_s} \dots \widehat{b}_{i_d, p_s} \mid i_l = 2, \dots, m_l - 1; l = 1, \dots, d \right\}. \end{aligned}$$

Analogously, the spline space with final and boundary conditions, in parametric coordinates, is

$$\begin{aligned} \widehat{\mathcal{X}}_{h,T} &:= \left\{ \widehat{v}_h \in \widehat{\mathcal{S}}_h^{\mathbf{p}} \mid \widehat{v}_h = 0 \text{ on } \{T\} \times \widehat{\Omega} \text{ and } \widehat{v}_h = 0 \text{ on } (0, 1) \times \partial\widehat{\Omega} \right\} \\ &= \widehat{\mathcal{X}}_{t, h_t, T} \otimes \widehat{\mathcal{X}}_{s, h_s} \end{aligned}$$

where

$$\widehat{\mathcal{X}}_{t, h_t, T} := \left\{ \widehat{w}_h \in \widehat{\mathcal{S}}_{h_t}^{p_t} \mid \widehat{w}_h(T) = 0 \right\} = \text{span} \left\{ \widehat{b}_{i_t, p_t} \mid i_t = 1, \dots, m_t - 1 \right\}.$$

More precisely, by reordering the basis functions, i.e. for the space with initial and boundary homogeneous conditions, we write

$$\begin{aligned}\widehat{\mathcal{X}}_{t,h_t,0} &= \text{span} \left\{ \widehat{b}_{i,p_t} \mid i = 1, \dots, n_t \right\}, \\ \widehat{\mathcal{X}}_{s,h_s} &= \text{span} \left\{ \widehat{b}_{i_1,p_s} \dots \widehat{b}_{i_d,p_s} \mid i_l = 1, \dots, n_{s,l}; l = 1, \dots, d \right\} \\ &= \text{span} \left\{ \widehat{B}_{i,p_s} \mid i = 1, \dots, N_s \right\},\end{aligned}$$

and then

$$\widehat{\mathcal{X}}_{h,0} = \text{span} \left\{ \widehat{B}_{i,p} \mid i = 1, \dots, N_{dof} \right\}, \quad (3.3)$$

where we defined  $n_t := m_t - 1$ ,  $n_{s,l} := m_l - 2$  for  $l = 1, \dots, d$ ,  $N_s := \prod_{l=1}^d n_{s,l}$  and  $N_{dof} := n_t N_s$ . We can proceed analogously with the space with final conditions.

Finally, the isogeometric space we consider is the isoparametric push-forward of (3.3) through the geometric map  $\mathbf{G}$ , i.e.

$$\mathcal{X}_{h,0} := \text{span} \left\{ B_{i,p} := \widehat{B}_{i,p} \circ \mathbf{G}^{-1} \mid i = 1, \dots, N_{dof} \right\}. \quad (3.4)$$

Notice that  $\mathcal{X}_{h,0} = \mathcal{X}_{t,h_t,0} \otimes \mathcal{X}_{s,h_s}$ , where

$$\mathcal{X}_{t,h_t,0} := \text{span} \left\{ b_{i,p_t} := \widehat{b}_{i,p_t}(\cdot/T) \mid i = 1, \dots, n_t \right\},$$

and

$$\mathcal{X}_{s,h_s} := \text{span} \left\{ B_{i,p_s} := \widehat{B}_{i,p_s} \circ \mathbf{F}^{-1} \mid i = 1, \dots, N_s \right\}.$$

Analogously, we define  $\mathcal{X}_{h,T}$ , the isogeometric space with homogeneous Dirichlet and final conditions.

### 3.3. Kronecker product

The Kronecker product of two matrices  $\mathbf{C} \in \mathbb{C}^{n_1 \times n_2}$  and  $\mathbf{D} \in \mathbb{C}^{n_3 \times n_4}$  is defined as

$$\mathbf{C} \otimes \mathbf{D} := \begin{bmatrix} [\mathbf{C}]_{1,1} \mathbf{D} & \dots & [\mathbf{C}]_{1,n_2} \mathbf{D} \\ \vdots & \ddots & \vdots \\ [\mathbf{C}]_{n_1,1} \mathbf{D} & \dots & [\mathbf{C}]_{n_1,n_2} \mathbf{D} \end{bmatrix} \in \mathbb{C}^{n_1 n_3 \times n_2 n_4},$$

where  $[\mathbf{C}]_{i,j}$  denotes the  $ij$ -th entry of the matrix  $\mathbf{C}$ . For extensions and properties of the Kronecker product we refer to [23]. In particular, when a matrix has a Kronecker product structure, the matrix-vector product can be efficiently computed. For this purpose, for  $m = 1, \dots, d+1$  we introduce the  $m$ -mode product of a tensor  $\mathfrak{X} \in \mathbb{C}^{n_1 \times \dots \times n_{d+1}}$  with a matrix  $\mathbf{J} \in \mathbb{C}^{\ell \times n_m}$ , that we denote by  $\mathfrak{X} \times_m \mathbf{J}$ . This is a tensor of size  $n_1 \times \dots \times n_{m-1} \times \ell \times n_{m+1} \times \dots \times n_{d+1}$ , whose elements are defined as

$$[\mathfrak{X} \times_m \mathbf{J}]_{i_1, \dots, i_{d+1}} := \sum_{j=1}^{n_m} [\mathfrak{X}]_{i_1, \dots, i_{m-1}, j, i_{m+1}, \dots, i_{d+1}} [\mathbf{J}]_{i_m, j}.$$

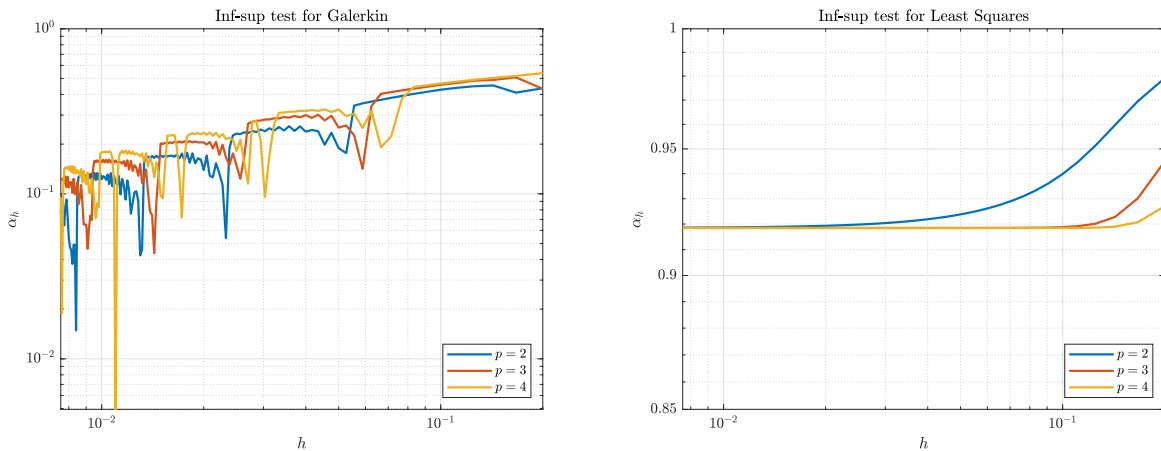
Then, given  $\mathbf{J}_i \in \mathbb{C}^{\ell_i \times n_i}$  for  $i = 1, \dots, d+1$ , it holds

$$(\mathbf{J}_{d+1} \otimes \dots \otimes \mathbf{J}_1) \text{vec}(\mathfrak{X}) = \text{vec}(\mathfrak{X} \times_1 \mathbf{J}_1 \times_2 \dots \times_{d+1} \mathbf{J}_{d+1}), \quad (3.5)$$

where the vectorization operator “vec” applied to a tensor stacks its entries into a column vector as

$$[\text{vec}(\mathfrak{X})]_j = [\mathfrak{X}]_{i_1, \dots, i_{d+1}} \text{ for } i_l = 1, \dots, n_l \text{ and for } l = 1, \dots, d+1,$$

where  $j := i_1 + \sum_{k=2}^{d+1} [(i_k - 1) \prod_{l=1}^{k-1} n_l]$ .



(A) Instability of space-time Galerkin method.

(B) Stability of space-time least squares method.

FIGURE 1. Inf-sup test for the space-time discretizations.

## 4. Space-time discretization of the Schrödinger equation

### 4.1. Instability of the space-time Galerkin method

Let  $\mathcal{V}_h := \mathcal{X}_{h,0}$  be the isogeometric space defined in (3.4) endowed with the  $\|\cdot\|_{\mathcal{V}}$ -norm, and choose  $\mathcal{W}_h := \mathcal{X}_{h,0}$  endowed with the  $\|\cdot\|_{\mathcal{W}}$ -norm. Consider the following Galerkin method for (2.2):

$$\text{Find } u_h \in \mathcal{V}_h \text{ such that } \mathcal{A}(u_h, w_h) = \mathcal{F}(w_h) \quad \forall w_h \in \mathcal{W}_h. \quad (4.1)$$

The stability and the well-posedness of formulation (4.1) are not guaranteed, indeed the inf-sup constant

$$\alpha_h := \inf_{v_h \in \mathcal{V}_h} \sup_{w_h \in \mathcal{W}_h} \frac{|\mathcal{A}(v_h, w_h)|}{\|v_h\|_{\mathcal{V}} \|w_h\|_{\mathcal{W}}} > 0,$$

depends on the mesh size  $h$  and degenerates under mesh refinement, as shown in Figure 1a.

### 4.2. Least squares space-time method

In order to retrieve a well posed space-time discretization to (2.2), notice that, given the quadratic functional  $\mathcal{J} : \mathcal{V} \rightarrow \mathbb{R}$ , defined as

$$\mathcal{J}(u) := \frac{1}{2} \|\mathbb{S}u - f\|_{L^2(\mathcal{Q})}^2,$$

we can write the least squares space-time formulation of (2.1): find  $u \in \mathcal{V}$  such that

$$u = \arg \min_{v \in \mathcal{V}} \mathcal{J}(v),$$

and its Euler-Lagrange equations are

$$(\mathbb{S}u, \mathbb{S}v) = (f, \mathbb{S}v), \quad \forall v \in \mathcal{V}.$$

This suggests to consider the following least-square discretization method for (2.2). Let  $\mathcal{V}_h := \mathcal{X}_{h,0}$  be the isogeometric space defined in (3.4) endowed with the  $\|\cdot\|_{\mathcal{V}}$ -norm, and choose  $\mathcal{W}_h := \mathbb{S}(\mathcal{V}_h)$  endowed with the  $\|\cdot\|_{\mathcal{W}}$ -norm. Consider the following Petrov-Galerkin approximation method for 2.2:

$$\text{Find } u_h \in \mathcal{V}_h \text{ such that } \mathcal{A}(u_h, w_h) = \mathcal{F}(w_h) \quad \forall w_h \in \mathcal{W}_h. \quad (4.2)$$

Notice that,  $\mathbb{S}$  is a bijection between the two discrete spaces, which means, for any  $h > 0$  it exists the inf-sup constant  $\underline{\alpha}_h > 0$ . Moreover, for this discretization, the inf-sup  $\alpha_h$  is uniformly bounded from below by a positive constant  $\alpha > 0$ , as it is investigated numerically in Figure 1b.

**Theorem 1.** *There exists a unique solution  $u_h \in \mathcal{V}_h$  to the discrete problem (4.2). Moreover, it holds*

$$\|u - u_h\|_{\mathcal{V}} \leq \frac{1}{\alpha} \inf_{v_h \in \mathcal{V}_h} \|u - v_h\|_{\mathcal{V}},$$

where  $u \in \mathcal{V}$  is the solution of (2.2).

We have then the following a-priori estimate for  $h$ -refinement.

**Theorem 2.** *Let  $q_t$  and  $q_s$  be two integers, such that  $q_t \geq 1$  and  $q_s \geq 2$ . If  $u \in \mathcal{V} \cap (H^{q_t}(0, T) \otimes H^2(\Omega)) \cap (H^1(0, T) \otimes H^{q_s}(\Omega))$  is the solution of (2.2) and  $u_h \in \mathcal{V}_h$  is the solution of (4.2), then it holds*

$$\|u - u_h\|_{\mathcal{V}} \leq C \left( h_t^{k_t-1} \|u\|_{H^{k_t}(0, T) \otimes H^2(\Omega)} + h_s^{k_s-2} \|u\|_{H^1(0, T) \otimes H^{k_s}(\Omega)} \right), \quad (4.3)$$

where  $k_t := \min\{q_t, p_t + 1\}$ ,  $k_s := \min\{q_s, p_s + 1\}$ , and  $C$  is a constant that depends only on  $p_t, p_s, \theta$  and the parametrization  $\mathbf{G}$ .

*Proof.* The result follows from the anisotropic error estimates developed in [24]. We report here only the main steps, since the proof is similar to the one of [15, Proposition 4]. The generalization of [24, Theorem 5.1] to the  $d + 1$  dimensional case, gives the existence of a projection  $\Pi_h : \mathcal{V} \cap (H^{q_t}(0, T) \otimes H^2(\Omega)) \cap (H^1(0, T) \otimes H^{q_s}(\Omega)) \rightarrow \mathcal{V}_h$ , such that

$$\begin{aligned} \|u - \Pi_h u\|_{L^2(0, T) \otimes L^2(\Omega)} &\leq C_1 \left( h_t^{k_t-1} \|u\|_{H^{k_t-1}(0, T) \otimes L^2(\Omega)} + h_s^{k_s-2} \|u\|_{L^2(0, T) \otimes H^{k_s-2}(\Omega)} \right), \\ \|u - \Pi_h u\|_{H^1(0, T) \otimes L^2(\Omega)} &\leq C_2 \left( h_t^{k_t-1} \|u\|_{H^{k_t}(0, T) \otimes L^2(\Omega)} + h_s^{k_s-2} \|u\|_{H^1(0, T) \otimes H^{k_s-2}(\Omega)} \right), \\ \|u - \Pi_h u\|_{L^2(0, T) \otimes H^2(\Omega)} &\leq C_3 \left( h_t^{k_t-1} \|u\|_{H^{k_t-1}(0, T) \otimes H^2(\Omega)} + h_s^{k_s-2} \|u\|_{L^2(0, T) \otimes H^{k_s}(\Omega)} \right). \end{aligned} \quad (4.4)$$

From the following inequality

$$\begin{aligned} \|u - v_h\|_{\mathcal{V}}^2 &= \|u - v_h\|_{L^2(\mathcal{Q})}^2 + \|\mathbb{S}(u - v_h)\|_{L^2(\mathcal{Q})}^2 \\ &\leq \|u - v_h\|_{L^2(\mathcal{Q})}^2 + 2\|\partial_t(u - v_h)\|_{L^2(\mathcal{Q})}^2 + 2\nu\|\Delta(u - v_h)\|_{L^2(\mathcal{Q})}^2 \\ &\leq \|u - v_h\|_{L^2(0, T) \otimes L^2(\Omega)}^2 + 2\|u - v_h\|_{H^1(0, T) \otimes L^2(\Omega)}^2 + 2\nu\|u - v_h\|_{L^2(0, T) \otimes H^2(\Omega)}^2, \end{aligned}$$

with the choice  $v_h = \Pi_h u$ , and by (4.4) with obvious upper bounds on the right hand side, it holds

$$\|u - \Pi_h u\|_{\mathcal{V}} \leq C \left( h_t^{k_t-1} \|u\|_{H^{k_t}(0, T) \otimes H^2(\Omega)} + h_s^{k_s-2} \|u\|_{H^1(0, T) \otimes H^{k_s}(\Omega)} \right),$$

therefore, (4.3) follows from Theorem 1.  $\square$

**Remark 1.** *In Theorem 1, the degrees  $p_t, p_s$  and the mesh-sizes  $h_t, h_s$  play a similar role. This motivates our choice  $p_t = p_s =: p$  and  $h_t = h_s =: h$  for the numerical tests in Section 6. In this case, and if the solution  $u$  is smooth, (4.3) yields  $h$ -convergence of order  $p - 1$ .*

### 4.3. Discrete system

The least-squares space-time discretization (4.2) can be written as:

$$\text{Find } u_h \in \mathcal{V}_h \text{ such that } \mathcal{A}(u_h, \mathbb{S}v_h) = \mathcal{F}(\mathbb{S}v_h) \quad \forall v_h \in \mathcal{V}_h,$$

and in particular, for all  $v_h \in \mathcal{V}_h$ , we point out that

$$\begin{aligned} \mathcal{A}(u_h, \mathbb{S}v_h) &= \int_{\Omega} \int_0^T (\mathbb{S}u_h) \overline{(\mathbb{S}v_h)} \, dt \, d\Omega \\ &= \int_{\Omega} \int_0^T \partial_t u_h \overline{\partial_t v_h} + \nu^2 \Delta u_h \overline{\Delta v_h} + i\nu \partial_t \nabla u_h \cdot \overline{\nabla v_h} - i\nu \nabla u_h \cdot \overline{\partial_t \nabla v_h} \, dt \, d\Omega, \end{aligned}$$

and

$$\mathcal{F}(\mathbb{S}v_h) = \int_{\Omega} \int_0^T f(\overline{\mathbb{S}v_h}) dt d\Omega = \int_{\Omega} \int_0^T f(\overline{i\partial_t v_h - \Delta v_h}) dt d\Omega.$$

Therefore, the linear system associated to (4.2) is

$$\mathbf{A}\mathbf{u} = \mathbf{f}, \quad (4.5)$$

where  $[\mathbf{A}]_{i,j} = \mathcal{A}(B_{j,\mathbf{p}}, \mathbb{S}(B_{i,\mathbf{p}}))$  and  $[\mathbf{f}]_i = \mathcal{F}(\mathbb{S}(B_{i,\mathbf{p}}))$ . The tensor-product structure of the isogeometric space (3.4) allows to write the system matrix  $\mathbf{A}$  as sum of Kronecker products of matrices as

$$\mathbf{A} = \mathbf{M}_s \otimes \mathbf{L}_t + \nu^2 \mathbf{B}_s \otimes \mathbf{M}_t + \nu \mathbf{L}_s \otimes (\mathbf{W}_t + \mathbf{W}_t^*), \quad (4.6)$$

where for  $i, j = 1, \dots, N_s$

$$\begin{aligned} [\mathbf{L}_s]_{i,j} &= \int_{\Omega} \nabla B_{i,p_s}(\mathbf{x}) \cdot \nabla B_{j,p_s}(\mathbf{x}) d\Omega, & [\mathbf{M}_s]_{i,j} &= \int_{\Omega} B_{i,p_s}(\mathbf{x}) B_{j,p_s}(\mathbf{x}) d\Omega, \\ [\mathbf{B}_s]_{i,j} &= \int_{\Omega} \Delta B_{i,p_s}(\mathbf{x}) \Delta B_{j,p_s}(\mathbf{x}) d\Omega. \end{aligned} \quad (4.7a)$$

while for  $i, j = 1, \dots, n_t$

$$\begin{aligned} [\mathbf{L}_t]_{i,j} &= \int_0^T b'_{j,p_t}(t) b'_{i,p_t}(t) dt, & [\mathbf{M}_t]_{i,j} &= \int_0^T b_{i,p_t}(t) b_{j,p_t}(t) dt, \\ [\mathbf{W}_t]_{i,j} &= i \int_0^T b'_{j,p_t}(t) b_{i,p_t}(t) dt, \end{aligned} \quad (4.7b)$$

#### 4.4. Ultraweak space-time method

Here we recall also the following ultraweak discretization that has been proposed in [9]. Let  $\mathcal{W}_h := \mathcal{X}_{h,T}$  be the isogeometric space with final conditions endowed with the  $\|\cdot\|_{\mathcal{W}}$ -norm, and fix  $\mathcal{V}_h := \mathbb{S}(\mathcal{W}_h)$  endowed with the  $\|\cdot\|_{L^2(\mathcal{Q})}$ -norm. Notice that,  $\forall v_h \in \mathcal{V}_h, w_h \in \mathcal{W}_h$ , it holds

$$\mathcal{A}(v_h, w_h) = (\mathbb{S}(v_h), w_h) = (v_h, \mathbb{S}(w_h)) - i(v_h(\cdot, 0), w_h(\cdot, 0))_{L^2(\Omega)},$$

with  $(\cdot, \cdot)_{L^2(\Omega)}$  denoting the complex scalar product in  $L^2(\Omega)$ . Therefore, introducing the sesquilinear form

$$\mathcal{A}_{\text{uw}}(v_h, w_h) := (v_h, \mathbb{S}(w_h)), \quad \forall v_h \in \mathcal{V}_h, w_h \in \mathcal{W}_h, \quad (4.8)$$

we have the following ultraweak method for (2.2):

$$\text{Find } u_h \in \mathcal{V}_h \text{ such that } \mathcal{A}_{\text{uw}}(u_h, w_h) = \mathcal{F}(w_h) + i(u_0, w_h(\cdot, 0))_{L^2(\Omega)} \quad \forall w_h \in \mathcal{W}_h, \quad (4.9)$$

where now the right hand side contains eventually the initial data  $u_0$ . As regards the well posedness and stability of (4.9) we refer to [9].

**Remark 2.** *The discrete system associated to (4.9) has the same Kronecker structure as (4.6), with appropriate final conditions at  $T$ .*

## 5. Fast solver for the parametric domain

In this section we focus on the case  $\mathbf{F} = Id$ , that is  $\mathcal{Q} = (0, T) \times (0, 1)^d$  is the parametric domain in space and a finite interval in time direction. In this context we are able to introduce a stable and fast solver for problem (4.2). We introduce, for the system (4.5), the preconditioner

$$\widehat{\mathbf{P}} := \widehat{\mathbf{M}}_s \otimes \mathbf{L}_t + \nu^2 \widehat{\mathbf{L}}_s^T \widehat{\mathbf{M}}_s^{-1} \widehat{\mathbf{L}}_s \otimes \mathbf{M}_t + \nu \widehat{\mathbf{L}}_s \otimes (\mathbf{W}_t + \mathbf{W}_t^*), \quad (5.1)$$



where the matrices  $\mathbf{L}_t, \mathbf{M}_t$  and  $\mathbf{W}_t$  are defined in (4.7b), while  $\widehat{\mathbf{L}}_s$  and  $\widehat{\mathbf{M}}_s$  are

$$\widehat{\mathbf{L}}_s = \sum_{l=1}^d \widehat{\mathbf{M}}_d \otimes \cdots \otimes \widehat{\mathbf{M}}_{l+1} \otimes \widehat{\mathbf{L}}_l \otimes \widehat{\mathbf{M}}_{l-1} \otimes \cdots \otimes \widehat{\mathbf{M}}_1, \quad \text{and} \quad \widehat{\mathbf{M}}_s = \widehat{\mathbf{M}}_d \otimes \cdots \otimes \widehat{\mathbf{M}}_1,$$

and for  $l = 1, \dots, d$ , with indexes  $i, j = 1, \dots, n_l$ , it holds

$$[\widehat{\mathbf{L}}_l]_{i,j} := \int_0^1 \widehat{b}'_{j,p}(x_l) \widehat{b}'_{i,p}(x_l) dx_l, \quad \text{and} \quad [\widehat{\mathbf{M}}_l]_{i,j} := \int_0^1 \widehat{b}_{j,p}(x_l) \widehat{b}_{i,p}(x_l) dx_l.$$

The efficient application of the proposed preconditioner, that is, the solution of a linear system with matrix  $\widehat{\mathbf{P}}$ , should exploit the structure highlighted above. When the pencils  $(\widehat{\mathbf{L}}_1, \widehat{\mathbf{M}}_1), \dots, (\widehat{\mathbf{L}}_d, \widehat{\mathbf{M}}_d)$  admit a stable generalized eigendecomposition, a possible approach is the Fast Diagonalization (FD) method, see [25] and [17] for details.

### 5.1. Stable factorization of $(\widehat{\mathbf{L}}_l, \widehat{\mathbf{M}}_l)$ for $l = 1, \dots, d$

The spatial stiffness and mass matrices  $\widehat{\mathbf{L}}_l$  and  $\widehat{\mathbf{M}}_l$  are symmetric and positive definite for  $l = 1, \dots, d$ . Thus, the pencils  $(\widehat{\mathbf{L}}_l, \widehat{\mathbf{M}}_l)$  for  $l = 1, \dots, d$  admit the generalized eigendecomposition

$$\widehat{\mathbf{L}}_l \mathbf{U}_l = \widehat{\mathbf{M}}_l \mathbf{U}_l \boldsymbol{\Lambda}_l,$$

where the matrices  $\mathbf{U}_l$  contain in each column the  $\widehat{\mathbf{M}}_l$ -orthonormal generalized eigenvectors and  $\boldsymbol{\Lambda}_l$  are diagonal matrices whose entries contain the generalized eigenvalues. Therefore we have for  $l = 1, \dots, d$  the factorizations

$$\mathbf{U}_l^T \widehat{\mathbf{L}}_l \mathbf{U}_l = \boldsymbol{\Lambda}_l \quad \text{and} \quad \mathbf{U}_l^T \widehat{\mathbf{M}}_l \mathbf{U}_l = \mathbb{I}_{n_{s,l}}, \quad (5.2)$$

where  $\mathbb{I}_{n_{s,l}}$  denotes the identity matrix of dimension  $n_{s,l} \times n_{s,l}$ . Figure 2 shows the shape of the generalized eigenvectors in  $\mathbf{U}_l$ , with associated eigenvalue in  $\boldsymbol{\Lambda}_l$ , for a fixed univariate direction  $l = 1, \dots, d$  discretized with degree  $p_s = 3$  B-Splines and uniform partition. The stability of the decomposition is expressed by the condition number of the eigenvector matrix. In particular  $\mathbf{U}_l^T \widehat{\mathbf{M}}_l \mathbf{U}_l = \mathbb{I}_{n_{s,l}}$  implies that

$$\kappa_2(\mathbf{U}_l) := \|\mathbf{U}_l\|_2 \|\mathbf{U}_l^{-1}\|_2 = \sqrt{\kappa_2(\widehat{\mathbf{M}}_l)},$$

where  $\|\cdot\|_2$  is the norm induced by the Euclidean vector norm. The condition number  $\kappa_2(\widehat{\mathbf{M}}_l)$  has been studied theoretically in [26] and numerically in [15] and it does not depend on the mesh-size, but it depends on the polynomial degree. Indeed, we report in Table 1 the behavior of  $\kappa_2(\mathbf{U}_l)$  for different values of spline degree  $p_s$  and for different uniform discretizations with number of elements denoted by  $n_{el}$ . We observe that  $\kappa_2(\mathbf{U}_l)$  exhibits a dependence only on  $p_s$ , but stays moderately low for all low polynomial degrees that are in the range of interest.

$n_{el}$	$p_s = 2$	$p_s = 3$	$p_s = 4$	$p_s = 5$	$p_s = 6$	$p_s = 7$	$p_s = 8$
32	$2.7 \cdot 10^0$	$4.5 \cdot 10^0$	$7.6 \cdot 10^0$	$1.3 \cdot 10^1$	$2.1 \cdot 10^1$	$3.5 \cdot 10^1$	$5.7 \cdot 10^1$
64	$2.7 \cdot 10^0$	$4.5 \cdot 10^0$	$7.6 \cdot 10^0$	$1.3 \cdot 10^1$	$2.1 \cdot 10^1$	$3.5 \cdot 10^1$	$5.7 \cdot 10^1$
128	$2.7 \cdot 10^0$	$4.5 \cdot 10^0$	$7.6 \cdot 10^0$	$1.3 \cdot 10^1$	$2.1 \cdot 10^1$	$3.5 \cdot 10^1$	$5.7 \cdot 10^1$
256	$2.7 \cdot 10^0$	$4.5 \cdot 10^0$	$7.6 \cdot 10^0$	$1.3 \cdot 10^1$	$2.1 \cdot 10^1$	$3.5 \cdot 10^1$	$5.7 \cdot 10^1$
512	$2.7 \cdot 10^0$	$4.5 \cdot 10^0$	$7.6 \cdot 10^0$	$1.3 \cdot 10^1$	$2.1 \cdot 10^1$	$3.5 \cdot 10^1$	$5.7 \cdot 10^1$
1024	$2.7 \cdot 10^0$	$4.5 \cdot 10^0$	$7.6 \cdot 10^0$	$1.3 \cdot 10^1$	$2.1 \cdot 10^1$	$3.5 \cdot 10^1$	$5.7 \cdot 10^1$

TABLE 1.  $\kappa_2(\mathbf{U}_l)$  for different polynomial degrees  $p_s$  and number of elements  $n_{el}$ .

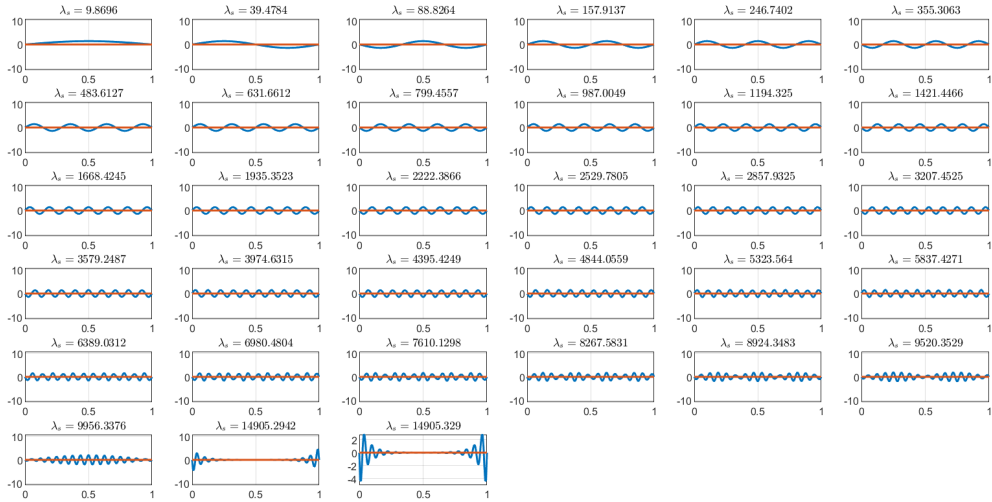


FIGURE 2. Generalized eigenvectors in space with associated eigenvalues for  $p_s = 3$  and  $n_{el} = 32$  elements. The real part is expressed in blue, while the imaginary part (null) is in red.

Moreover, in [27] it is shown that there is spectral equivalence between  $\widehat{\mathbf{B}}_s$  and  $\widehat{\mathbf{L}}_s^T \widehat{\mathbf{M}}_s^{-1} \widehat{\mathbf{L}}_s$ . We investigate numerically this spectral equivalence, and Figure 3a shows the eigenvalues of  $(\widehat{\mathbf{L}}_s^T \widehat{\mathbf{M}}_s^{-1} \widehat{\mathbf{L}}_s)^{-1} \widehat{\mathbf{B}}_s$  are clustered and close to 1, for splines of degree  $p = 2, 3, 4$  and different uniform partitionas with  $n_{el} = 8, 16, 32, 64, 128$ . In conclusion the spectral equivalence is stable under mesh refinement.

As regards the time pencils, the spectral equivalence between  $\widehat{\mathbf{L}}_t$  and  $\widehat{\mathbf{W}}_t^* \widehat{\mathbf{M}}_t^{-1} \widehat{\mathbf{W}}_t$  is unstable under mesh refinement, see Figure 3b where we performed the analogous test, therefore we kept the full structure of the time pencils in the preconditioner.

## 5.2. Application of the preconditioner

The application of the preconditioner involves the solution of the linear system

$$\widehat{\mathbf{P}}\mathbf{s} = \mathbf{r}, \quad (5.3)$$

where  $\widehat{\mathbf{P}}$  has the structure (5.1). We are able to efficiently solve system (5.3) by the Fast Diagonalization method. The starting point, is the setup of the preconditioner, that is the factorizations (5.2) of the pencils  $(\widehat{\mathbf{L}}_l, \widehat{\mathbf{M}}_l)$  for  $l = 1, \dots, d$ .

Then, define  $\mathbf{U}_s := \mathbf{U}_d \otimes \dots \otimes \mathbf{U}_1$  and  $\mathbf{\Lambda}_s := \sum_{l=1}^d \mathbb{I}_{n_{s,d}} \otimes \dots \otimes \mathbb{I}_{n_{s,l+1}} \otimes \mathbf{\Lambda}_l \otimes \mathbb{I}_{n_{s,l-1}} \otimes \dots \otimes \mathbb{I}_{n_{s,1}}$ . Notice that  $\widehat{\mathbf{M}}_s^{-1} = \mathbf{U}_s \mathbf{U}_s^T$ , therefore the matrix  $\widehat{\mathbf{L}}_s \widehat{\mathbf{M}}_s^{-1} \widehat{\mathbf{L}}_s$  admits the stable factorization

$$\mathbf{U}_s^T \widehat{\mathbf{L}}_s \widehat{\mathbf{M}}_s^{-1} \widehat{\mathbf{L}}_s \mathbf{U}_s = \mathbf{\Lambda}_s^2.$$

The preconditioner  $\widehat{\mathbf{P}}$  admits the following factorization

$$\widehat{\mathbf{P}} = (\mathbf{U}_s^T \otimes \mathbb{I}_{n_t})^{-1} (\mathbb{I}_{N_s} \otimes \mathbf{L}_t + \nu^2 \mathbf{\Lambda}_s^2 \otimes \mathbf{M}_t + \nu \mathbf{\Lambda}_s \otimes (\mathbf{W}_t + \mathbf{W}_t^*)) (\mathbf{U}_s \otimes \mathbb{I}_{n_t})^{-1}. \quad (5.4)$$

Note that the second factor in (5.4) that is

$$\mathbf{H} := (\mathbb{I}_{N_s} \otimes \mathbf{L}_t + \nu^2 \mathbf{\Lambda}_s^2 \otimes \mathbf{M}_t + \nu \mathbf{\Lambda}_s \otimes (\mathbf{W}_t + \mathbf{W}_t^*))$$

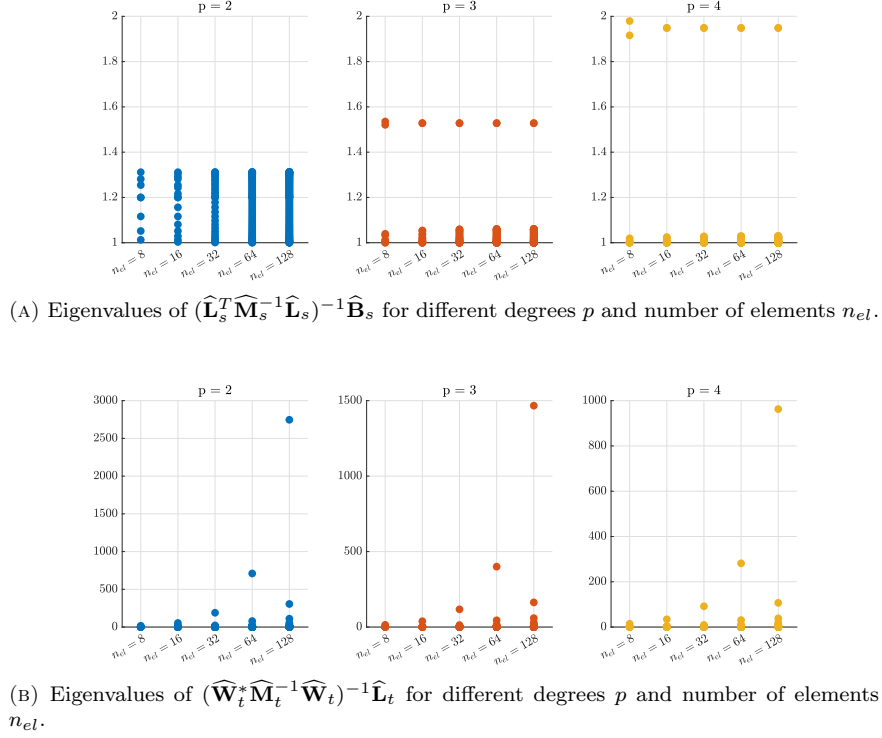


FIGURE 3. Numerical investigation of spectral equivalence.

is sum of three Kronecker matrices, whose space factors are diagonal matrices. We have the following block diagonal structure

$$\mathbf{H} = \begin{bmatrix} \mathbf{H}_1 & & & \\ & \ddots & & \\ & & \ddots & \\ & & & \mathbf{H}_{N_s} \end{bmatrix},$$

where  $\mathbf{H}_i$ , for  $i = 1, \dots, N_s$ , are banded matrices with bandwidth  $2p_t + 1$  defined as

$$\mathbf{H}_i := \mathbf{L}_t + \nu^2 [\mathbf{A}_s^2]_{i,i} \mathbf{M}_{n_t} + \nu [\mathbf{A}_s]_{i,i} (\mathbf{W}_t + \mathbf{W}_t^*).$$

In order to invert  $\mathbf{H}$ , it is now sufficient to invert the following independent  $N_s$  problems of size  $n_t \times n_t$ :

$$\mathbf{H}_i \mathbf{x}_i = \mathbf{y}_i \quad \text{for } i = 1, \dots, N_s. \quad (5.5)$$

Summarizing, the solution of (5.3) can be computed by the following algorithm.

---

**Algorithm 1** Fast Diagonalization

---

- 1: Compute the factorizations (5.2).
  - 2: Compute  $\mathbf{y} = (\mathbf{U}_s^T \otimes \mathbb{I}_t) \mathbf{r}$ .
  - 3: Compute  $\mathbf{x}_i = \mathbf{H}_i^{-1} \mathbf{y}_i$  for  $i = 1, \dots, N_s$ .
  - 4: Compute  $\mathbf{s} = (\mathbf{U}_s \otimes \mathbb{I}_t) \tilde{\mathbf{s}}$ .
- 

We conclude with the following remark for a possible parallel implementation of Algorithm 1.

**Remark 3.** *The decision to consider time as the first variable allows us to write the matrix  $\mathbf{H}$  in a block diagonal form. In view of an efficient parallel implementation, this natural diagonal block structure does not require data shuffling, decreasing the communication cost between nodes.*

### 5.3. Computational cost and memory requirements

In this section we discuss the computational costs and memory requirements in the implementation of Algorithm 1. First, notice that the matrix  $\mathbf{A}$  in (4.6) is symmetric positive definite therefore we choose Conjugate Gradients (CG) as linear solver for solving the system (4.5). Clearly, the computational cost of each iteration of the CG solver depends on both the preconditioner setup and application cost.

We assume for simplicity that, for each univariate direction  $l = 1, \dots, d$ , the space matrices have dimension  $n_s \times n_s$ , while the time matrices involved in the preconditioners, have dimension  $n_t \times n_t$ . Thus the total number of degrees-of-freedom is  $N_{dof} = N_s n_t = n_s^d n_t$ .

The setup of  $\hat{\mathbf{P}}$  includes the operations performed in Step 1 of Algorithm 1, i.e.  $d$  spatial eigendecompositions, that have a total cost of  $O(dn_s^3)$  FLOPs, and the construction of the block diagonal matrix  $\mathbf{H}$ , which costs  $O(p_t n_t N_s) = O(p_t N_{dof})$ . We remark that the setup of the preconditioners has to be performed only once, since the matrices involved do not change during the iterative procedure.

The application of the preconditioner is performed by Steps 2-4 of Algorithm 1. Exploiting (3.5), Step 2 and Step 4 costs  $O(dn_s^{d+1}n_t) = O(dn_s N_{dof})$  FLOPs. The cost of solving each sparse problem (5.5) makes the cost for Step 3 equal to  $O(p_t^2 n_t N_s) = O(p_t^2 N_{dof})$  FLOPs.

In conclusion, the total cost of Algorithm 1 is  $O(dn_s^3) + O(dn_s N_{dof}) + O(p_t^2 N_{dof})$  FLOPs. The non-optimal dominant cost of Step 2 and Step 4 is determined by the dense matrix-matrix products. However, these operations are usually implemented on modern computers in a very efficient way and the overall serial computational time grows almost as  $O(N_{dof})$ , see i.e. [15, 16]

The other dominant computational cost in a CG iteration is the cost of the residual computation. In Algorithm 1, this involves the multiplication of the matrix  $\mathbf{A}$  with a vector. This multiplication is done by exploiting the special structure (4.6), that allows a matrix-free approach and the use of formula (3.5). With the matrix-free approach, noting that the time matrices  $\mathbf{L}_t, \mathbf{M}_t, \mathbf{W}_t$  are banded matrices with bandwidth  $2p_t + 1$ , and the spatial matrices  $\mathbf{J}_s, \mathbf{L}_s, \mathbf{M}_s$  have a number of non-zeros per row equal to  $(2p_s + 1)^d$ , the computational cost of a single matrix-vector product is  $O(N_{dof} p^d)$  FLOPs, if we assume  $p = p_s \approx p_t$ . The dominant cost in the iterative solver is represented by the residual computation. This is a typical behaviour of the FD-based preconditioning strategies, see [15, 28, 29].

We now investigate the memory consumption of the preconditioning strategy proposed. For the preconditioner, we have to store the eigenvector spatial matrices,  $\mathbf{U}_1, \dots, \mathbf{U}_d$ , the diagonal matrices  $\mathbf{\Lambda}_1, \dots, \mathbf{\Lambda}_d$  and the banded time pencils  $\mathbf{L}_t, \mathbf{M}_t$  and  $\mathbf{W}_t$  of size  $n_t \times n_t$ . The memory required is roughly

$$O(d(n_s^2 + n_s)) + O(p_t N_{dof}) + O(p_t n_t).$$

For the system matrix  $\mathbf{A}$ , in addition to the time factors  $\mathbf{L}_t, \mathbf{M}_t$  and  $\mathbf{W}_t$ , we need to store the spatial factors  $\mathbf{M}_s, \mathbf{B}_s$  and  $\mathbf{L}_s$ . Thus the memory further required is roughly

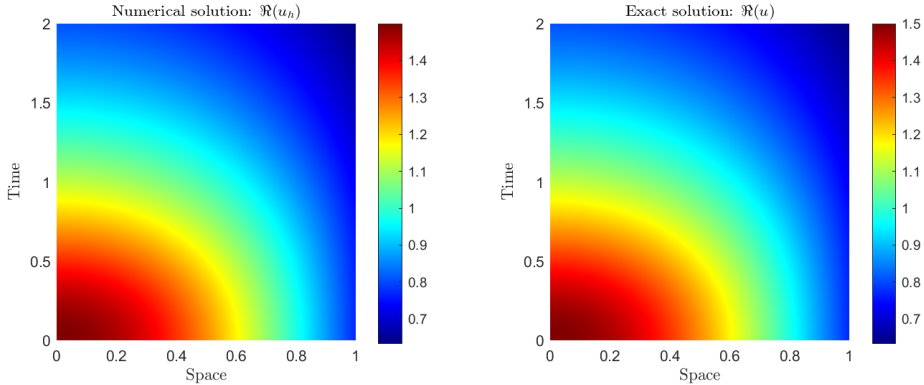
$$O(p_s^d N_s).$$

These numbers show that memory-wise our space-time strategy is very appealing when compared to other approaches, even when space and time variables are discretized separately, e.g., with finite differences in time or other time-stepping schemes. For example if we assume  $d = 3$ ,  $p_t \approx p_s = p$  and  $n_t^2 \leq Cp^3 N_s$ , then the total memory consumption is  $O(p^3 N_s + N_{dof})$ , that is equal to the sum of the memory needed to store the Galerkin matrices associated to spatial variables and the memory needed to store the solution of the problem.

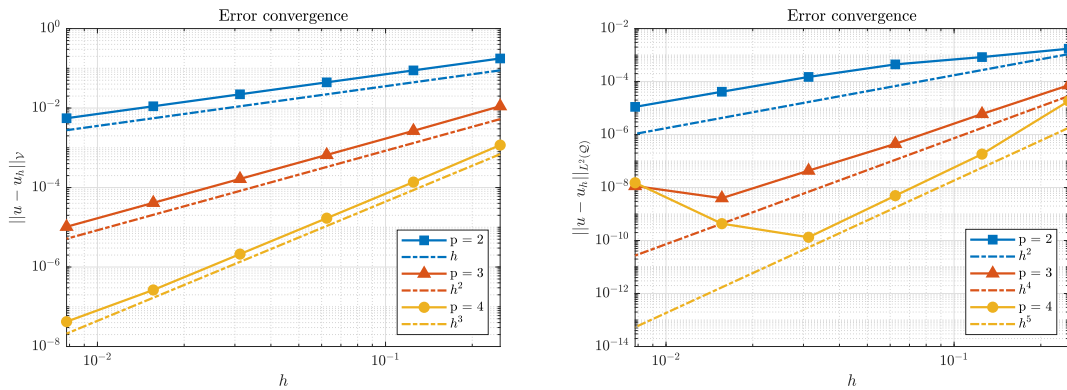
We remark that we could avoid storing the factors of  $\mathbf{A}$  by using the matrix-free approach of [14]. The memory and the computational cost of the iterative solver would significantly improve, both for the setup and the matrix-vector multiplications. However, we do not pursue this strategy, as it is beyond the scope of this paper.

## 6. Numerical Results

This section is devoted to the computation of the solution of Schrödinger problem (2.1), and to its extension to non-homogeneous conditions, with the discretization proposed in (4.2). We first present the numerical



(A) *Left* - Real part of the smooth gaussian solution computed with space-time splines discretization of degree  $p = 3$ , over a uniform mesh with 64 elements in space and 128 elements in time. *Right* - Real part of the exact solution.



(B) Error convergence in  $\mathcal{V}$ -norm.

(C) Error convergence in  $L^2(\mathcal{Q})$ -norm.

FIGURE 4. Smooth solution and error convergence of the space-time least squares discretization.

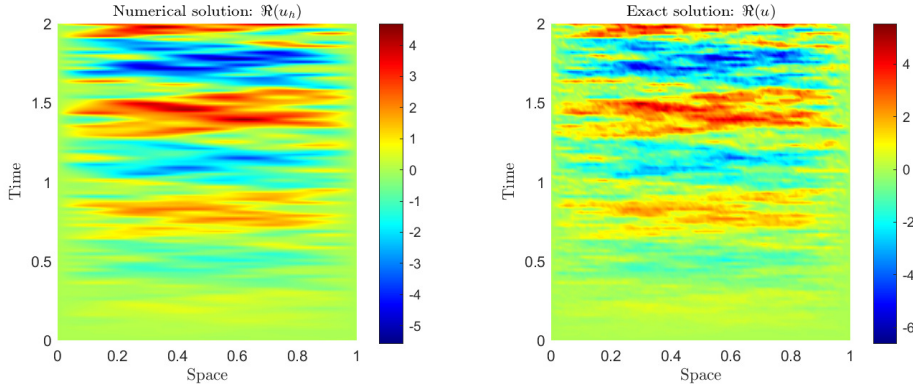
experiments that assess the convergence behavior of the least squares Petrov-Galerkin approximation and then we analyze the performance of the preconditioners.

We consider only sequential executions and we force the use of a single computational thread in a Intel Core i5-1035G1 processor, running at 1 GHz and with 16 GB of RAM.

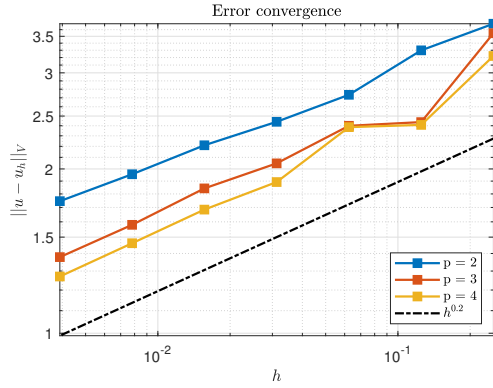
The tests are performed with Matlab R2023a and GeoPDEs toolbox [30]. We use the `eig` Matlab function to compute the generalized eigendecompositions present in Step 1 of Algorithm 1, while Tensorlab toolbox [31] is employed to perform the multiplications with Kronecker matrices occurring in Step 2 and Step 4. The solution of the linear systems (5.5) in Step 3 is performed pagewise by Matlab direct solver (pagewise backslash operator `pagemldivide`). The linear system is solved by CG, with tolerance equal to  $10^{-8}$  and with the null vector as initial guess in all tests.

According to Remark 1, we use the same mesh-size in space and in time  $h_s = h_t =: h$ , and use splines of maximal continuity and same degree in space and in time  $p_t = p_s =: p$ . For the sake of simplicity, we also consider uniform knot vectors, and denote the number of elements in each parametric direction by  $n_{el} := \frac{1}{h}$ .

In our tables, the symbol “\* \*” denotes that the inversion of the matrix  $\mathbf{A}$  in (4.6), by Matlab direct solver backslash operator “\”, requires more than 2 hours of computational time, while the symbol “\*” indicates that the number of iterations in the CG solver exceeds the upper bound set to 200 iterates. We remark that in all the tables the total solving time of the iterative strategies includes also the setup time of the considered preconditioner.



(A) *Left* - Real part of the non-regular solution computed with space-time splines discretization of degree  $p = 4$ , over a uniform mesh with 512 elements in space and 1024 elements in time. *Right* - Real part of the exact solution.



(B) Error convergence in  $\mathcal{V}$ -norm.

FIGURE 5. Non-regular solution and error convergence of the space-time discretization.

### 6.1. Orders of convergence

Consider the Schrödinger equation as modeled in (2.1), for the space time domain  $\mathcal{Q} = (0, T) \times (0, 1)$ , with  $T = 2$ . The reference solution is the complex gaussian

$$u(t, x) = \frac{\alpha\beta}{\sqrt{\beta^2 - i\gamma t}} \exp\left\{-\frac{x^2}{\beta^2 - i\gamma t}\right\}, \quad (6.1)$$

where  $\alpha = \beta = 1.5$  and  $\gamma = 2.5$ . Here the Dirichlet boundary condition is  $u|_{\Gamma_D}$ , the initial condition is  $u(0, x)$  and the right hand side is  $f = Au$ . The problem is discretized with a uniform mesh in both space and time directions. The solution for  $p = 3$  is shown in Figure 4a. In Figure 4b it is shown the convergence analysis of the error under  $h$ -refinement and for different polynomial degrees, for instance  $p = 2, \dots, 4$ . The errors are computed both with  $\|\cdot\|_{\mathcal{V}}$ -norm, for which the convergence Theorem 1 holds, and with  $\|\cdot\|_{L^2(\mathcal{Q})}$ -norm, even if this case is not covered by theoretical results. For this smooth solution, the error study reveals optimal convergence under  $h$ -refinement in  $\mathcal{V}$ -norm, and the  $L^2(\mathcal{Q})$  error is lower than the residual component in the  $\mathcal{V}$ -norm.

The second test considers the following example from [7]. Consider the space domain  $\Omega = (0, 1)$ , the final time  $T = 2$ , and the space-time domain  $\mathcal{Q} = (0, T) \times (0, 1)$ . Homogeneous Dirichlet boundary conditions are considered on  $\Gamma_D$ . Let us denote by  $e_k$  and  $\omega_k^2$ , which is, for  $k = 1, 2, \dots$ , an eigenpair of

$$-\Delta e_k = \omega_k^2 e_k, \quad \text{a.e. in } \Omega.$$

By normalizing  $e_k$  such that  $\|e_k\|_{L^2(\Omega)} = 1$ , we consider  $f(t, x) = \sum_{k=1}^{+\infty} f_k(t)e_k(x)$ , where  $f_k(t)$  are the Fourier coefficients of  $f$  decomposed in the orthonormal basis  $e_k$  at a given time  $t$ . By the following specific choice of coefficients

$$f_k(t) = \frac{1}{k} \exp \{i\omega_k^2 t\} \quad \text{for } k = 1, 2, \dots,$$

we considered as right hand side in (2.1) the following high mode truncated expansion

$$f_M = \sum_{k=1}^M \frac{1}{k} \exp \{i\omega_k^2 t\} e_k(x),$$

with  $M \gg 0$ . Notice that, the solution to (2.1) with this specific right-hand side, is

$$u(t, x) = \sum_{k=1}^M \frac{-it}{k} \exp \{i\omega_k^2 t\} e_k(x).$$

We computed the solution for different polynomial degrees, on a uniform mesh, for an high mode right hand side  $f_M$ , with  $M = 625$ . In 5a it is plotted the real part of the numerical solution for splines with degree  $p = 4$ , together with the real part of the explicit solution. The solution of such a problem is non-regular and it can be shown that  $u(t, \cdot) \in H^{1/2}(\Omega)$ , while  $u(\cdot, x) \in H^{1/4}(0, T)$ . Figure 5b shows the error convergence for the high mode right hand side  $f_M$ , with  $M = 652$  modes, that is optimal for each polynomial degree  $p = 2, 3, 4$ .

## 6.2. Performance of the preconditioner in the parametric domain

The computational space domain is  $\Omega = (0, 1)^2$  and the space time domain is  $\mathcal{Q} = (0, T) \times \Omega$  with  $T = 1$ . The reference solution is a traveling wave, that is

$$u(t, \mathbf{x}) = a \exp \left\{ -i \frac{|\mathbf{x}|^2 + t^2}{\omega^2} \right\}, \quad (6.2)$$

with wave number  $\omega = 0.2$  and amplitude  $a = \sqrt[4]{2/\omega^2}$ . Here the Dirichlet boundary conditions are  $u|_{\Gamma_D}$ . The right hand side is the following

$$f(t, \mathbf{x}) = a \left( \frac{4i}{\omega^2} + \frac{4|\mathbf{x}|^2}{\omega^4} + \frac{2t}{\omega^2} \right) \exp \left\{ -i \frac{|\mathbf{x}|^2 + t^2}{\omega^2} \right\}.$$

The numerical solution on a mesh of 64 elements per univariate direction is shown in Figure 6 for different time frames.

We analyze the performance of the proposed preconditioner  $\widehat{\mathbf{P}}$  for a variety of uniform partitions up to  $n_{el} = 64$  per univariate directions, and polynomial degree  $p = 2, 3, 4$ . In Table 2 it is reported the computational clock time cost of solving the linear system both directly using Matlab backslash and iteratively by CG solver, reporting also the number of iterations for this latter case. When solving with CG we investigate the performance of the solver with preconditioner  $\widehat{\mathbf{P}}$ , and compare it with a classical algebraic preconditioner as incomplete Cholesky factorization (ICHOL). Matlab backslash is clearly inefficient, since performing gaussian elimination requires  $N_{dof}^3$  FLOPs. Using classical preconditioners in CG iterative solvers is a reasonable approach for small size problem, but the number of iterations grows with the size of the problem. The performance of the preconditioner  $\widehat{\mathbf{P}}$  with CG, is identical among  $h$ -refined meshes, and seems reasonably  $p$ -robust. The number of iterations never exceeds 10, and the total amount of time required to solve the discrete problem, is always cheaper than the other approaches we tested.

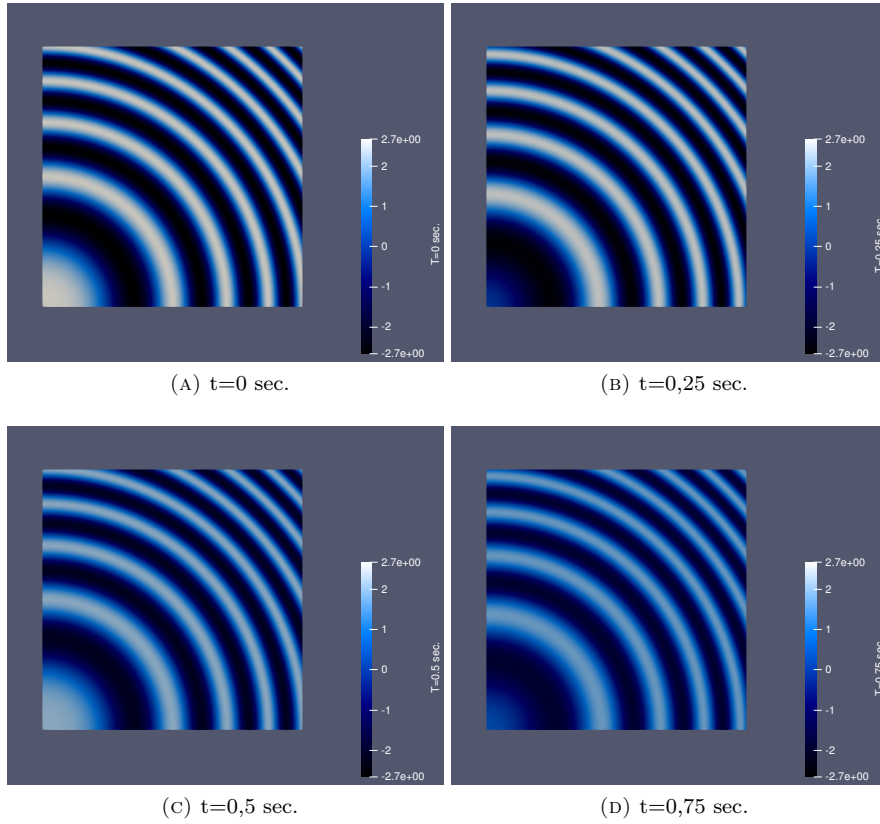


FIGURE 6. Real part of the numerical approximation of (6.2) at four different time frames.

TABLE 2. Parametric domain. Performance of  $\widehat{\mathbf{P}}$ .

Performance of preconditioner				
$N_e$	$N_{dof}$	backslash (time)	$\widehat{\mathbf{P}}$ (iter / time)	ICHOL (iter / time)
Degree $p = 2$				
8	1000	0.0306	7 / 0.0426	12 / 0.0256
16	5832	0.7974	7 / 0.0659	38 / 0.1338
32	39304	27.46	7 / 0.2992	174 / 3.9153
64	287496	1148	7 / 2.7304	*
Degree $p = 3$				
8	1331	0.0618	8 / 0.0302	10 / 0.0172
16	6859	1.6415	9 / 0.0982	32 / 0.2884
32	42875	118	8 / 0.4703	148 / 8.1482
64	300763	**	8 / 4.7142	*
Degree $p = 4$				
8	1728	0.1587	10 / 0.0427	10 / 0.0548
16	8000	2.6433	10 / 0.2289	28 / 0.4363
32	46656	419	10 / 1.2329	127 / 14.1742
64	314432	**	10 / 9.0219	191 / 176



## 7. Conclusions

In this work we proposed and studied a space-time least square method for the Schrödinger equation in the framework of isogeometric analysis. Our scheme is based on smooth spline in space and time, that allows, in the particular case of the parametric domain, to introduce a suitable preconditioner for the arising linear system. Our preconditioner  $\widehat{\mathbf{P}}$  is represented by a sum of Kronecker products of matrices, that makes the computational cost of its construction (setup) and application, as well as the storage cost, very appealing. In particular the construction of the preconditioner exploits a spectral equivalence between the space matrices  $\mathbb{B}_s$  and  $\mathbf{L}_s^T \mathbf{M}_s^{-1} \mathbf{L}_s$  that, thanks to the FD technique, admits a stable block-diagonal factorization.

The application cost for a serial execution is almost equal to  $O(N_{dof})$ , and the block-diagonal structure is suitable for parallel implementation on distributed memory machines, and this will be an interesting future direction of study.

At the same time, the storage cost is roughly the same that we would have by discretizing separately in space and in time, if we assume  $n_t \leq Cp^d N_s$ . Indeed, in this case the memory used for the whole iterative solver is  $O(p^d N_s + N_{dof})$ . Although, our approach could be coupled with a matrix-free idea, and this is expected to further improve the efficiency of the overall method.

As a final comment, it would be interesting to further exploits the structure of time pencils, in order to achieve a full factorization of the proposed preconditioner. This may also give a hint in proposing an ad-hoc preconditioner for the isogeometric framework, which we are still working on.

## Appendix A. Well-posedness of the space-time variational formulation

Here we extend the results presented in [7] on the well posedness of (2.2). First we introduce a suitable notation, such that this appendix can be read independently from the paper. Let us recall  $\mathcal{Q} = (0, T) \times \Omega$ , with  $\Omega \subset \mathbb{R}^d$ ,  $d = 1, 2, 3$ , while  $\Gamma_D = (0, T) \times \partial\Omega$ . Consider  $\Gamma_0 = \Gamma_D \cup (\{0\} \times \Omega)$  and  $\Gamma_T = \Gamma_D \cup (\{T\} \times \Omega)$  and let us define  $\mathcal{D}_0 := \{\phi \in C_0^\infty(\mathbb{R}^{d+1}) : \phi|_{\Gamma_0} = 0\}$ , which is the space of smooth functions of  $\mathbb{R}^{d+1}$  with compact support such that restricted to  $\mathcal{Q}$  satisfy both homogeneous Dirichlet and initial conditions. Analogously define  $\mathcal{D}_T := \{\psi \in C_0^\infty(\mathbb{R}^{d+1}) : \psi|_{\Gamma_T} = 0\}$ , that instead satisfies homogeneous Dirichlet and final conditions. Recall  $\mathbb{S} := i\partial_t - \nu\Delta$ , and notice that integration by parts gives:

$$\int_{\Omega} \int_0^T (\mathbb{S}\phi) \bar{\psi} \, dt \, d\Omega = \int_{\Omega} \int_0^T \phi (\overline{\mathbb{S}\psi}) \, dt \, d\Omega, \quad \forall \phi \in \mathcal{D}_0, \text{ and } \forall \psi \in \mathcal{D}_T.$$

The space  $\mathcal{V}$  in (2.2) is the domain of  $\mathbb{S} : \mathcal{V} \subset L^2(\mathcal{Q}) \rightarrow L^2(\mathcal{Q})$ , that can be written as:

$$\mathcal{V} := \{v \in L^2(\mathcal{Q}) : \mathbb{S}v \in L^2(\mathcal{Q}) \text{ and } (\mathbb{S}v, v) - (v, \mathbb{S}v) = 0 \, \forall v \in \mathcal{D}_T\}, \quad (\text{A.1})$$

and we have  $\mathcal{C}_0^\infty(\mathcal{Q}) \subset \mathcal{V} \subset L^2(\mathcal{Q})$ , that is  $\mathbb{S}$  is densely defined. Denoting by  $\mathbb{S}^* : \mathcal{V}^* \subset L^2(\mathcal{Q}) \rightarrow L^2(\mathcal{Q})$  the adjoint operator, whose domain is given by

$$\mathcal{V}^* := \{w \in L^2(\mathcal{Q}) : \exists g \in L^2(\mathcal{Q}) \text{ such that } (\mathbb{S}v, w) = (v, g) \, \forall v \in \mathcal{V}\}, \quad (\text{A.2})$$

we have  $\mathbb{S}^*w := g$ , with  $\mathbb{S}^* = \mathbb{S}$ , and  $\mathcal{C}_0^\infty(\mathcal{Q}) \subset \mathcal{V}^* \subset L^2(\mathcal{Q})$ . Notice that we are identifying  $L^2(\mathcal{Q})' \equiv L^2(\mathcal{Q})$  through Riesz isomorphism. We endow both  $\mathcal{V}$  and  $\mathcal{V}^*$  with the norms  $\|\cdot\|_{\mathcal{V}}$  and  $\|\cdot\|_{\mathcal{V}^*}$  respectively, such that

$$\|v\|_{\mathcal{V}}^2 := \|v\|_{L^2(\mathcal{Q})}^2 + \|\mathbb{S}v\|_{L^2(\mathcal{Q})}^2, \quad \text{and} \quad \|v\|_{\mathcal{V}^*}^2 := \|v\|_{L^2(\mathcal{Q})}^2 + \|\mathbb{S}^*v\|_{L^2(\mathcal{Q})}^2.$$

Define the boundary operators  $B : \mathcal{V} \rightarrow (\mathcal{V}^*)'$  and  $B^* : \mathcal{V}^* \rightarrow (\mathcal{V})'$ , such that

$$\langle Bv, w \rangle := (\mathbb{S}v, w)_{L^2(\mathcal{Q})} - (v, \mathbb{S}^*w)_{L^2(\mathcal{Q})}, \quad (\text{A.3a})$$

$$\langle B^*w, v \rangle := (\mathbb{S}^*w, v)_{L^2(\mathcal{Q})} - (w, \mathbb{S}v)_{L^2(\mathcal{Q})}, \quad (\text{A.3b})$$

hold true for all  $v, w \in L^2(\mathcal{Q})$  such that  $\mathbb{S}v, \mathbb{S}^*w \in L^2(\mathcal{Q})$ . From [7, Lemma A.2], we have

$$\mathcal{V}^* = (B(\mathcal{V}))^\perp, \quad (\text{A.4})$$

and, from (A.1), it holds

$$\mathcal{V} = (B^*(\mathcal{D}_T))^\perp. \quad (\text{A.5})$$

In particular, from [7, Lemma 2.1], it holds  $\mathcal{D}_0 \subset \mathcal{V}$  and  $\mathcal{D}_T \subset \mathcal{V}^*$ , and in addition we make the following density assumption.

**Assumption 4.** We assume that  $\overline{\mathcal{D}_0}^{\|\cdot\|_{\mathcal{V}}} = \mathcal{V}$  and  $\overline{\mathcal{D}_T}^{\|\cdot\|_{\mathcal{V}^*}} = \mathcal{V}^*$ .

Under Assumption 4, from [7, Lemma 2.2], it holds

$$\mathcal{V}^* = (B(\mathcal{V}))^\perp = (B(\mathcal{D}_0))^\perp, \quad (\text{A.6})$$

and

$$\mathcal{V} = (B^*(\mathcal{V}^*))^\perp = (B^*(\mathcal{D}_T))^\perp. \quad (\text{A.7})$$

The next result states the well posedness of the space time variational formulation.

**Theorem 3.** Under Assumption 4, the linear Schrödinger operator  $\mathbb{S} : \mathcal{V} \rightarrow L^2(\mathcal{Q})$  is a continuous bijections, that is problem (2.2) is well posed.

The proof of well posedness is given in [7, Theorem 2.4], and Assumption 4, but more precisely (A.6), is needed only to prove injectivity of  $\mathbb{S}$ . We now prove that, Assumption (4) is verified for every integer  $d \geq 1$ .

**Lemma 1.** Given  $\mathcal{Q} = (0, T) \times \Omega$ , with  $\Omega = [0, 1]^d$  and integer  $d \geq 1$ , then Assumption (4) holds true.

*Proof.* We prove that  $\mathcal{D}_0$  is dense in  $\mathcal{V}$ , the other stated density result is analogous. The case  $d = 1$  is in [7, Theorem 3.1], thus we fix an integer  $d > 1$ . Consider  $v \in \mathcal{V}$ , first we extend  $v$  to the whole  $\mathbb{R}^{d+1}$  domain.

1. *Extending along space directions:* Let us extend the space-time domain among the space directions as follows. Denote by  $\mathcal{Q}_{1,c} = \mathcal{Q}$ ,  $\mathcal{Q}_{1,l} := [0, T] \times [-1, 0] \times [0, 1]^{d-1}$  and  $\mathcal{Q}_{1,r} := [0, T] \times [1, 2] \times [0, 1]^{d-1}$ . Analogously, for  $i = 2, \dots, d$ , we introduce  $\mathcal{Q}_{i,c} := \bigcup_{j \in \{l, c, r\}} \mathcal{Q}_{i-1,j}$ , then  $\mathcal{Q}_{i,l} := [0, T] \times [-1, 2]^{i-1} \times [-1, 0] \times [0, 1]^{d-i}$  and  $\mathcal{Q}_{i,r} := [0, T] \times [-1, 2]^{i-1} \times [1, 2] \times [0, 1]^{d-i}$ , considering  $[0, 1]^0 = \emptyset$ . Finally let us call  $\Omega_E := \bigcup_{j \in \{l, c, r\}} \mathcal{Q}_{d,j}$  the enlarged space-time cylinder. Then, we introduce the intermediate extension operators,  $E_i : \mathcal{Q}_{i,c} \rightarrow \mathcal{Q}_{i+1,c}$  for  $i = 1, \dots, d-1$ , and  $E_d : \mathcal{Q}_{d,c} \rightarrow \mathcal{Q}_E$ , such that

$$E_i f(t, \mathbf{x}) := \begin{cases} -f(t, x_1, \dots, -x_i, \dots, x_d) & (t, \mathbf{x}) \in \mathcal{Q}_{i,l}, \\ f(t, x_1, \dots, x_i, \dots, x_d) & (t, \mathbf{x}) \in \mathcal{Q}_{i,c}, \\ -f(t, x_1, \dots, 2 - x_i, \dots, x_d) & (t, \mathbf{x}) \in \mathcal{Q}_{i,r}. \end{cases}$$

We denote the reverse operators by  $E'_i$ , defined as  $E'_i g(t, \mathbf{x}) = g(t, \mathbf{x}) - g(t, x_1, \dots, -x_i, \dots, x_d) - g(t, x_1, \dots, 2 - x_i, \dots, x_d)$ , for  $(t, \mathbf{x}) \in \mathcal{Q}_{i,c}$ , and for  $i = 1, \dots, d$ . The definitions are to be interpreted almost everywhere, and finally our extension operator from  $\mathcal{Q}$  to  $\mathcal{Q}_E$  is  $E := E_d \circ \dots \circ E_1$ , while its reverse operator from  $\mathcal{Q}_E$  to  $\mathcal{Q}$  is  $E' = E'_1 \circ \dots \circ E'_d$ . It is easy to see by a change of variable that

$$(Ef, g)_{L^2(\mathcal{Q}_E)} = (f, E'g)_{L^2(\mathcal{Q})}, \quad \forall f \in L^2(\mathcal{Q}), \forall g \in L^2(\mathcal{Q}_E).$$

Next, we claim that

$$\mathbb{S}Ev = E\mathbb{S}v, \quad \forall v \in \mathcal{V}.$$

Clearly,  $Ev$  is in  $L^2(\mathcal{Q}_E)$  and notice that  $E'\mathbb{S}\varphi = \mathbb{S}E'\varphi$  for all  $\varphi \in C_0^\infty(\mathcal{Q}_E)$ . Therefore, it holds

$$\begin{aligned} \langle \mathbb{S}Ev, \varphi \rangle_{C_0^\infty(\mathcal{Q}_E)} &= (Ev, \mathbb{S}\varphi)_{L^2(\mathcal{Q}_E)} = (v, E'\mathbb{S}\varphi)_{L^2(\mathcal{Q})} = \\ &= (v, \mathbb{S}E'\varphi)_{L^2(\mathcal{Q})} = (\mathbb{S}v, E'\varphi)_{L^2(\mathcal{Q})} - \langle Bv, E'\varphi \rangle. \end{aligned}$$

Now, since  $E'\varphi|_{\Gamma_T} = 0$ , we have  $E'\varphi \in \mathcal{V}^*$ , and thus  $\langle Bv, E'\varphi \rangle = 0$  by (A.4). It follows that

$$\langle \mathbb{S}Ev, \varphi \rangle_{C_0^\infty(\mathcal{Q}_E)} = (\mathbb{S}v, E'\varphi)_{L^2(\mathcal{Q})} = (E\mathbb{S}v, E\varphi)_{L^2(\mathcal{Q}_E)},$$

completing the proof of the claim. We also conclude that  $\mathbb{S}Ev$  is in  $L^2(\mathcal{Q}_E)$  whenever  $v \in \mathcal{V}$ .

2. *Extending along time direction:* Let  $\tilde{E}$  denote the extension of  $E$  by zero to  $\mathbb{R}^{d+1}$ , and  $\tau_\delta$  be the translation operator in  $t$  direction, i.e.,  $\tau_\delta w(t, \mathbf{x}) = w(t - \delta, \mathbf{x})$ . From [32] it holds

$$\lim_{\delta \rightarrow 0} \|\tau_\delta w - w\|_{L^2(\mathbb{R}^{d+1})} = 0, \quad \forall w \in L^2(\mathbb{R}^{d+1}). \quad (\text{A.8})$$

Introducing  $\mathcal{Q}_{E,\delta} = (-\delta, T + \delta) \times (-1, 2)^d$ , by a change of variables, it holds

$$(\tau_\delta \tilde{E}f, g)_{L^2(\mathcal{Q}_{E,\delta})} = (Ef, \tau_{-\delta}g)_{L^2(\mathcal{Q}_E)}, \quad \forall f \in L^2(\mathcal{Q}), \forall g \in L^2(\mathcal{Q}_{E,\delta}).$$

Denoting by  $R_\delta$  the restriction operator of function on  $\mathbb{R}^{d+1}$  to  $\mathcal{Q}_{E,\delta}$ , we now claim that

$$\mathbb{S}R_\delta \tau_\delta \tilde{E}v = R_\delta \tau_\delta \tilde{E}\mathbb{S}v, \quad \forall v \in \mathcal{V}.$$

The proof is analogous to the one in Step 1. Given  $\varphi \in C_0^\infty(\mathcal{Q}_{E,\delta})$  it holds

$$\begin{aligned} \langle \mathbb{S}R_\delta \tau_\delta \tilde{E}v, \varphi \rangle_{C_0^\infty(\mathcal{Q}_{E,\delta})} &= (\tau_\delta \tilde{E}v, \mathbb{S}\varphi)_{L^2(\mathcal{Q}_{E,\delta})} = (Ev, \mathbb{S}\tau_{-\delta}\varphi)_{L^2(\mathcal{Q}_E)} \\ &= (v, E'\mathbb{S}\tau_{-\delta}\varphi)_{L^2(\mathcal{Q})} = (v, \mathbb{S}E'\tau_{-\delta}\varphi)_{L^2(\mathcal{Q})} \\ &= (\mathbb{S}v, E'\tau_{-\delta}\varphi)_{L^2(\mathcal{Q})} - \langle Bv, E'\tau_{-\delta}\varphi \rangle. \end{aligned}$$

Now, since  $E'\tau_{-\delta}\varphi|_{\Gamma_T} = 0$ , we have  $E'\tau_{-\delta}\varphi \in \mathcal{V}^*$ , and thus  $\langle Bv, E'\tau_{-\delta}\varphi \rangle = 0$  by (A.4). It follows that

$$\langle \mathbb{S}R_\delta \tau_\delta \tilde{E}v, \varphi \rangle_{C_0^\infty(\mathcal{Q}_{E,\delta})} = (\tilde{E}\mathbb{S}v, \tau_{-\delta}\varphi)_{L^2(\mathcal{Q}_E)} = (\tau_{-\delta}\tilde{E}\mathbb{S}v, \varphi)_{L^2(\mathcal{Q}_{E,\delta})},$$

which proves the claim.

3. *Mollify:* Consider the mollifier  $\rho_\epsilon \in C_0^\infty(\mathbb{R}^{d+1})$ , defined by

$$\rho_\epsilon(t, \mathbf{x}) := \epsilon^{-d-1} \rho_1(\epsilon^{-1}t, \epsilon^{-1}x_1, \dots, \epsilon^{-1}x_d), \quad \text{for } \epsilon > 0,$$

where

$$\rho_1(t, \mathbf{x}) := \begin{cases} ke^{-1/(1-|(t,\mathbf{x})|^2)}, & \text{if } |(t,\mathbf{x})|^2 < 1, \\ 0 & \text{if } |(t,\mathbf{x})|^2 \geq 1, \end{cases}$$

with  $|\cdot|$  denoting the Euclidean norm in  $\mathbb{R}^{d+1}$ , and  $k$  is a constant chosen such that  $\int_{\mathbb{R}^{d+1}} \rho_1 = 1$ . Notice that, given  $\delta > 0$  small enough, i.e.,  $\delta < \min\{T/2, 1/2\}$ , the convolutions  $v_\epsilon := \rho_\epsilon * \tau_\delta \tilde{E}v$  and  $s_\epsilon := \rho_\epsilon * \tau_\delta \tilde{E}\mathbb{S}v$  are smooth functions that satisfy

$$\lim_{\epsilon \rightarrow 0} \|v_\epsilon - \tau_\delta \tilde{E}v\|_{L^2(\mathbb{R}^{d+1})} = 0, \quad \text{and} \quad \lim_{\epsilon \rightarrow 0} \|s_\epsilon - \tau_\delta \tilde{E}\mathbb{S}v\|_{L^2(\mathbb{R}^{d+1})} = 0. \quad (\text{A.9})$$

Moreover, the smooth function  $\mathbb{S}v_\epsilon$  need not coincide to  $s_\epsilon$  everywhere, but they coincide on  $\mathcal{Q}$  whenever  $\epsilon < \delta/2$ . Thus, consider  $\delta = 3\epsilon$ , and let  $\epsilon < \min\{T/6, 1/6\}$  go to zero. We have

$$\|\mathbb{S}v_\epsilon - \mathbb{S}v\|_{L^2(\mathcal{Q})} = \|s_\epsilon - \mathbb{S}v\|_{L^2(\mathcal{Q})} \leq \|s_\epsilon - \tau_\delta \tilde{E}\mathbb{S}v\|_{L^2(\mathbb{R}^{d+1})} + \|\tau_\delta \tilde{E}\mathbb{S}v - \tilde{E}\mathbb{S}v\|_{L^2(\mathbb{R}^{d+1})}$$

and

$$\|v_\epsilon - v\|_{L^2(\mathcal{Q})} \leq \|v_\epsilon - \tau_\delta \tilde{E}v\|_{L^2(\mathcal{Q})} + \|\tau_\delta \tilde{E}v - \tilde{E}v\|_{L^2(\mathcal{Q})}$$

Using (A.8) and (A.9), it follows that

$$\lim_{\epsilon \rightarrow 0} \|v_\epsilon - v\|_{\mathcal{V}} = 0.$$

To conclude, we examine the value of  $v_\epsilon$  at the edges of the space-time cylinder. We have

$$v_\epsilon(t, 0, x_2, \dots, x_d) = \int_{\mathbb{R}^{d+1}} \rho_\epsilon(t - \sigma, -r_1, x_2 - r_2, \dots, x_d - r_d) \tau_\delta \tilde{E}v(\sigma, r_1, \dots, r_d) dr_1 \dots dr_d d\sigma,$$

with the integrand the inner integral being the product of an even function  $\rho_\epsilon$ , with respect to  $r_1$ , and an odd function  $\tau_\delta \tilde{E}v$  of  $r_1$ . Thus  $v_\epsilon(t, 0, x_2, \dots, x_d) = 0$  and the same holds for  $v_\epsilon(t, 1, x_2, \dots, x_d)$  and the other univariate space directions. Moreover since  $\tau_\delta \tilde{E}v$  is identically zero in a neighborhood of  $(0, \mathbf{x})$ , we conclude that  $v_\epsilon|_{\Gamma_0} = 0$ .

□

Next we extend this result to the isogeometric case domain.

**Theorem 4.** *Given  $\mathcal{Q} = (0, T) \times \Omega$ , with  $\Omega = \mathbf{F}([0, 1]^d)$  and integer  $d \geq 1$ , then Assumption (4) holds true.*

*Proof.* We prove that  $\mathcal{D}_0$  is dense in  $\mathcal{V}$ , the other stated density result is analogous. Given  $v \in \mathcal{V}$ , recall  $\mathbf{G} : [0, 1]^{d+1} \rightarrow \mathcal{Q}$  is the parameterization of the space-time cylinder, such that  $\mathbf{G}(\tau, \boldsymbol{\eta}) := (T\tau, \mathbf{F}(\boldsymbol{\eta})) = (t, \mathbf{x})$ . Define  $\widehat{v} := v \circ \mathbf{G}$ . Clearly  $\widehat{v} \in L^2([0, 1]^{d+1})$ , and  $\mathbb{S}\widehat{v} \in L^2([0, 1]^{d+1})$ . Moreover  $(\mathbb{S}v, \phi)_{L^2([0, 1]^{d+1})} - (v, \mathbb{S}\phi)_{L^2([0, 1]^{d+1})} = 0$ , for all  $\phi \in \mathcal{C}_0^\infty(\mathbb{R}^{d+1})$  such that  $\phi|_{\mathbf{G}^{-1}(\Gamma_T)} = 0$ . By applying Lemma 1, it exists  $\{\widehat{v}_\epsilon\}_{\epsilon>0} \subset \mathcal{C}_0^\infty(\mathbb{R}^{d+1})$  such that  $\widehat{v}_\epsilon|_{\mathbf{G}^{-1}(\Gamma_0)} = 0$ , that satisfies

$$\lim_{\epsilon \rightarrow 0} \|\widehat{v}_\epsilon - \widehat{v}\|_{L^2([0, 1]^{d+1})}^2 + \|\mathbb{S}\widehat{v}_\epsilon - \mathbb{S}\widehat{v}\|_{L^2([0, 1]^{d+1})}^2 = 0.$$

Therefore define  $v_\epsilon := \widehat{v}_\epsilon \circ \mathbf{G}^{-1}$  and notice that  $\{v_\epsilon\}_{\epsilon>0} \subset \mathcal{D}_0$ . Moreover, by a change of variable,

$$\lim_{\epsilon \rightarrow 0} \|v_\epsilon - v\|_{\mathcal{V}}^2 \leq C \lim_{\epsilon \rightarrow 0} \|\widehat{v}_\epsilon - \widehat{v}\|_{L^2([0, 1]^{d+1})}^2 + \|\mathbb{S}\widehat{v}_\epsilon - \mathbb{S}\widehat{v}\|_{L^2([0, 1]^{d+1})}^2 = 0.$$

This completes the proof. □

## Acknowledgments

## References

- [1] I. Fried, Finite-element analysis of time-dependent phenomena., AIAA Journal 7 (6) (1969) 1170–1173.
- [2] J. C. Bruch Jr., G. Zyzolowski, Transient two-dimensional heat conduction problems solved by the finite element method, International Journal for Numerical Methods in Engineering 8 (3) (1974) 481–494.
- [3] J. T. Oden, A general theory of finite elements. I. Topological considerations, International Journal for Numerical Methods in Engineering 1 (2) (1969) 205–221.
- [4] J. T. Oden, A general theory of finite elements. II. Applications, International Journal for Numerical Methods in Engineering 1 (3) (1969) 247–259.
- [5] F. Shakib, T. J. R. Hughes, A new finite element formulation for computational fluid dynamics: IX. Fourier analysis of space-time Galerkin/least-squares algorithms, Computer Methods in Applied Mechanics and Engineering 87 (1) (1991) 35–58.
- [6] O. Karakashian, C. Makridakis, A space-time finite element method for the nonlinear Schrödinger equation: the discontinuous Galerkin method, Mathematics of computation 67 (222) (1998) 479–499.
- [7] L. Demkowicz, J. Gopalakrishnan, S. Nagaraj, P. Sepulveda, A spacetime DPG method for the Schrödinger equation, SIAM Journal on Numerical Analysis 55 (4) (2017) 1740–1759.
- [8] S. Gómez, A. Moiola, A space-time Trefftz discontinuous Galerkin method for the linear Schrödinger equation, SIAM Journal on Numerical Analysis 60 (2) (2022) 688–714.
- [9] S. Hain, K. Urban, An ultra-weak space-time variational formulation for the Schrödinger equation, arXiv preprint arXiv:2212.14398 (2022).
- [10] T. J. R. Hughes, J. A. Cottrell, Y. Bazilevs, Isogeometric analysis: CAD, finite elements, NURBS, exact geometry and mesh refinement, Computer Methods in Applied Mechanics and Engineering 194 (39) (2005) 4135–4195.
- [11] J. A. Cottrell, T. J. R. Hughes, Y. Bazilevs, Isogeometric analysis: toward integration of CAD and FEA, John Wiley & Sons, 2009.
- [12] J. A. Evans, Y. Bazilevs, I. Babuška, T. J. R. Hughes,  $n$ -widths, sup-infs, and optimality ratios for the  $k$ -version of the isogeometric finite element method, Computer Methods in Applied Mechanics and Engineering 198 (2009) 1726–1741.
- [13] A. Bressan, E. Sande, Approximation in FEM, DG and IGA: a theoretical comparison, Numerische Mathematik (2019).
- [14] G. Sangalli, M. Tani, Matrix-free weighted quadrature for a computationally efficient isogeometric  $k$ -method, Computer Methods in Applied Mechanics and Engineering 338 (2018) 117 – 133.
- [15] M. Montardini, M. Negri, G. Sangalli, M. Tani, Space-time least-squares isogeometric method and efficient solver for parabolic problems, Mathematics of Computation (accepted for publication) (2019).
- [16] G. Loli, M. Montardini, G. Sangalli, M. Tani, An efficient solver for space–time isogeometric Galerkin methods for parabolic problems, Computers & Mathematics with Applications 80 (11) (2020) 2586–2603.
- [17] R. E. Lynch, J. R. Rice, D. H. Thomas, Direct solution of partial difference equations by tensor product methods, Numerische Mathematik 6 (1) (1964) 185–199.
- [18] C. A. Dorao, H. A. Jakobsen, A parallel time–space least-squares spectral element solver for incompressible flow problems, Applied Mathematics and Computation 185 (1) (2007) 45–58.
- [19] M. J. Gander, 50 years of time parallel time integration, in: Multiple Shooting and Time Domain Decomposition Methods, Springer, 2015, pp. 69–113.

- [20] A. M. Kvarving, E. M. Rønquist, A fast tensor-product solver for incompressible fluid flow in partially deformed three-dimensional domains: Parallel implementation, *Computers & Fluids* 52 (2011) 22–32.
- [21] L. C. Evans, *Partial Differential equations*, American Mathematical Society, Berlin, 2010.
- [22] C. De Boor, *A practical guide to splines (revised edition)*, Applied Mathematical Sciences, Springer, Berlin, 2001.
- [23] T. G. Kolda, B. W. Bader, Tensor decompositions and applications, *SIAM review* 51 (3) (2009) 455–500.
- [24] L. Beirão da Veiga, D. Cho, G. Sangalli, Anisotropic NURBS approximation in isogeometric analysis, *Computer Methods in Applied Mechanics and Engineering* 209 (2012) 1–11.
- [25] M. O. Deville, P. F. Fischer, E. H. Mund, *High-order methods for incompressible fluid flow*, Cambridge University Press, 2002.
- [26] K. P. S. Gahalaut, S. K. Tomar, C. Douglas, Condition number estimates for matrices arising in NURBS based isogeometric discretizations of elliptic partial differential equations, *arXiv preprint arXiv:1406.6808* (2014).
- [27] J. Henning, D. Palitta, V. Simoncini, K. Urban, An ultraweak space-time variational formulation for the wave equation: Analysis and efficient numerical solution, *ESAIM: Mathematical Modelling and Numerical Analysis* 56 (4) (2022) 1173–1198.
- [28] G. Sangalli, M. Tani, Isogeometric preconditioners based on fast solvers for the Sylvester equation, *SIAM Journal on Scientific Computing* 38 (6) (2016) A3644–A3671.
- [29] M. Montardini, G. Sangalli, M. Tani, Robust isogeometric preconditioners for the Stokes system based on the Fast Diagonalization method, *Computer Methods in Applied Mechanics and Engineering* 338 (2018) 162 – 185.
- [30] R. Vázquez, A new design for the implementation of isogeometric analysis in Octave and Matlab: GeoPDEs 3.0, *Computers & Mathematics with Applications* 72 (3) (2016) 523–554.
- [31] L. Sorber, M. Van Barel, L. De Lathauwer, *Tensorlab v2. 0*, Available online, URL: [www.tensorlab.net](http://www.tensorlab.net) (2014).
- [32] H. Brezis, *Functional analysis, Sobolev spaces and partial differential equations*, Vol. 2, Springer, 2011.